LIMNOLOGY AND OCEANOGRAPHY
Letters

ASLO
Open Access

Limnology and Oceanography Letters 10, 2025, 37–61
© 2024 The Author(s). *Limnology and Oceanography Letters* published by Wiley Periodicals LLC on behalf of Association for the Sciences of Limnology and Oceanography.
doi: 10.1002/lol2.10447

DATA ARTICLE

The Great Lakes Winter Grab: Limnological data from a multi-institutional winter sampling campaign on the Laurentian Great Lakes

Ge Pu[1] *Kirill Shchapov*[2] *Nolan J. T. Pearce*[3] *Kelly Bowen*[4] *Andrew Bramburger*[5] *Andrew Camilleri*[6] *Hunter Carrick*[7] *Justin D. Chaffin*[8] *William Cody*[9] *Maureen L. Coleman*[10] *Warren J. S. Currie*[4] *David C. Depew*[11] *Jonathan P. Doubek*[12,13] *Rachel Eveleth*[14] *Mark Fitzpatrick*[4] *Paul W. Glyshaw*[15] *Casey M. Godwin*[6] *R. Michael McKay*[16] *Mohiuddin Munawar*[4] *Heather Niblock*[4] *Maci Quintanilla*[17] *Michael Rennie*[18,19] *Matthew W. Sand*[20] *Kimberly J. Schraitle*[20] *Michael R. Twiss*[21] *Donald G. Uzarski*[20] *Henry A. Vanderploeg*[15] *Trista J. Vick-Majors*[17] *Judy A. Westrick*[22] *Bridget A. Wheelock*[20] *Marguerite A. Xenopoulos*[3] *Arthur Zastepa*[11] *Ted Ozersky*[23]*

[1]Cleveland Water Alliance, Cleveland, Ohio, USA; [2]Cawthron Institute, Nelson, New Zealand; [3]Department of Biology, Trent University, Peterborough, Ontario, Canada; [4]Great Lakes Laboratory for Fisheries and Aquatic Sciences, Fisheries and Oceans Canada, Burlington, Ontario, Canada; [5]Watershed Hydrology and Ecology Research Division, Water Science and Technology Directorate, Environment and Climate Change Canada, Burlington, Ontario, Canada; [6]Cooperative Institute for Great Lakes Research, University of Michigan, Ann Arbor, Michigan, USA; [7]Department of Biology, Institute for Great Lakes Research, Central Michigan University, Mt. Pleasant, Michigan, USA; [8]F.T. Stone Laboratory, The Ohio State University, Put-in-Bay, Ohio, USA; [9]Aquatic Taxonomy Specialists, Malinta, Ohio, USA; [10]Department of the Geophysical Sciences, University of Chicago, Chicago, Illinois, USA; [11]Environment and Climate Change Canada, Science and Technology Branch, Burlington, Ontario, Canada; [12]School of Natural Resources, Lake Superior State University, Sault Sainte Marie, Michigan, USA; [13]Center for Freshwater Research and Education, Lake Superior State University, Sault Sainte Marie, Michigan, USA; [14]Department of Geosciences, Oberlin College, Oberlin, Ohio, USA; [15]NOAA Great Lakes Environmental Research Laboratory, Ann Arbor, Michigan, USA; [16]Great Lakes Institute for Environmental Research, University of Windsor, Windsor, Ontario, Canada; [17]Department of Biological Sciences, Michigan Technological University, Houghton, Michigan, USA; [18]Department of Biology, Lakehead University, Thunder Bay, Ontario, Canada; [19]IISD Experimental Lakes Area, Winnipeg, Manitoba, Canada; [20]CMU Biological Station and Department of Biology, Institute for Great Lakes Research, Central Michigan University, Mt. Pleasant, Michigan, USA; [21]Department of Biology, Algoma University, Sault Ste Marie, Ontario, Canada; [22]Lumigen Instrument Center, Wayne State University, Detroit, Michigan, USA; [23]Large Lakes Observatory, University of Minnesota Duluth, Duluth, Minnesota, USA

*Correspondence: tozersky@d.umn.edu

Associate editor: Kendra Spence Cheruvelil

Author Contribution Statement: GP and TO wrote most of the manuscript text with contributions from AB, HC, WC, WJSC, DD, MF, RMM, MM, NJTP, MRT, TJV-M, WW, MAX, AZ for method information. GP led data management and QA/QC efforts, as well as deposition of data in data repositories. KS directed field and sample analysis coordination and logistics. KS, NJTP, GP, and TO analyzed data. KS, NJTP, KB, AB, AC, JDC, WC, DD, JPD, RE, PWG, CG, RMM, HN, MQ, MR, MRT, HAV, TJV-M, MAX, AZ participated in field operations. KS, NJTP, KB, HC, WC, MLC, DD, RE, MF, CMG, RMM, HN, TO, MQ, MRT, WW, MAX, AZ, performed sample analysis. NJTP and TO created figs. AB, AC, HC, JDC, MLC, WJSC, DD, JPD, RE, MF, PWG, CMG, RMM, MM, HN, TO, NJTP, MR, MRT, HAV, TJV-M, MAX, AZ contributed to conception or design of the project. TO directed the overall project. All co-authors read and contributed to editing the paper.

Data Availability Statement: Data are available in the Environmental Data Initiative repository at https://doi.org/10.6073/pasta/ab6702bee340e64033c1d672f03876ac.

This is an open access article under the terms of the Creative Commons Attribution License, which permits use, distribution and reproduction in any medium, provided the original work is properly cited.

Scientific Significance Statement

Winter remains an understudied season in the annual cycle of lakes. This is especially true for the world's largest lakes, where challenging winter conditions and size make systematic winter study difficult. Studying winter limnology is important because it addresses ecosystem functioning during an understudied period of the year and could help improve predictions of environmental responses to climate change. In this data paper, we describe a dataset generated during the 2022 Great Lakes Winter Grab—a collaborative sampling campaign that sampled 49 locations throughout all five of the Laurentian Great Lakes and some of their connecting waters. We report data on ice and snow characteristics as well as diverse physical, biogeochemical, and biological parameters, making this the most extensive dataset of winter observations for the Great Lakes. These data will be of interest to aquatic scientists as a baseline of Great Lakes winter conditions during a period of rapid climate change, to enable comparisons with other systems and times of the year, and for integration of these data into cross-system synthesis efforts.

Abstract

Interest in winter limnology is growing rapidly, but progress is hindered by a shortage of standardized multivariate datasets on winter conditions. Addressing the winter data gap will enhance our understanding of winter ecosystem function and of lake response to environmental change. Here, we describe a dataset generated by a multi-institutional winter sampling campaign across all five Laurentian Great Lakes and some of their connecting waters (the Great Lakes Winter Grab). The objective of Winter Grab was to characterize mid-winter limnological conditions in the Great Lakes using standard sample collection and analysis methods. Nineteen research groups sampled 49 locations varying widely in depth and trophic status, collecting a range of limnological data. This dataset includes physical, chemical, and biological measurements. These data can be used to examine diverse aspects of Great Lakes ecosystems or integrated with winter observations from other lakes to improve understanding of winter limnology across different aquatic systems.

Background and motivation

Climate change is having profound and diverse impacts on Earth's lakes. Among these impacts are decreased ice cover duration or the complete disappearance of winter ice on seasonally freezing lakes (Sharma et al. 2019; Wang et al. 2022). Rapidly changing winter conditions and the need to understand and forecast their impacts on lakes have highlighted limnology's "winter knowledge gap": the great majority of limnological research has focused on the open water seasons, leaving the ice cover period understudied in comparison (Salonen et al. 2009; Hampton et al. 2017). Studying winter in lakes is important because winter processes can significantly influence the function of lake ecosystems, including nutrient cycling, oxygen dynamics, as well as biological population and community structure (Farmer et al. 2015; Hampton et al. 2017; Yang et al. 2020; Shchapov and Ozersky 2023). Better understanding of winter conditions will help predict how lakes respond to ongoing climate changes and for developing effective ecosystem management strategies (Knoll et al. 2019; Dugan 2021).

Recognition of the winter knowledge gap is spurring limnologists to rapidly increase their efforts to understand the winter ecology of diverse lakes and to integrate winter into full-year models of lake ecosystem function. Dozens of studies focusing on winter limnology were published over the past decade, focusing on physical, chemical, and biological observations and on attempts to integrate these observations into conceptual frameworks (e.g., Kirillin et al. 2012; Twiss et al. 2012; Beall et al. 2016; Hampton et al. 2017; Cavaliere et al. 2021; Dugan 2021; Jensen et al. 2021; Weyhenmeyer et al. 2022).

While critical to filling the "winter knowledge gap," much of contemporary work on winter limnology is focused on relatively narrow topics (e.g., aspects of physics, biogeochemistry, or biology) and on small spatial scales, often characterizing a few sites in a single lake or a small number of lakes. Additionally, most recent winter limnology research has concentrated on relatively small lakes with stable and predictable ice cover. Much less winter research has been conducted on the Laurentian Great Lakes, which are characterized by large spatial and interannual variation in ice cover conditions, as well as large gradients in trophic status and other limnological conditions (Sterner et al. 2017; Ozersky et al. 2021). The size of the Great Lakes and their severe winter conditions have impeded systematic winter study of their ecosystem, resulting in an especially acute winter knowledge gap (Ozersky et al. 2021). The relatively few existing winter studies on the Laurentian Great Lakes have revealed that their winter ecology and biogeochemistry are dramatically different from those of other seasons and are linked to ecosystem function during the rest of the year (Eadie et al. 2002; Twiss et al. 2012; Farmer

et al. 2015; Reavie et al. 2016; Doan et al. 2018; Shchapov and Ozersky 2023). As the largest freshwater ecosystem in the world, the Laurentian Great Lakes provide ecosystem services to millions of people in the United States, Canada, and over 185 Indigenous nations and communities in the Great Lakes basin (Serville-Tertullien et al. 2023). Moreover, the Great Lakes serve as a unique natural laboratory, encompassing scales and processes found in both smaller freshwater lakes and marine systems (Sterner et al. 2017). Thus, understanding their winter dynamics is an important priority.

Collaborative, multi-institutional sampling campaigns enable researchers to overcome challenges associated with sampling across large spatial scales and allow collection of data on many more locations and parameters than an individual investigator team could address. The Lake Erie HABs Grab (Chaffin et al. 2021) is a recent example of this approach that involved eight institutions from both the US and Canada, and many more groups have utilized the HABs Grabs data as a result of this collaboration. We used a similar approach (which we call "The Great Lakes Winter Grab," or simply "Winter Grab") to collect winter-period samples across the Great Lakes. Our sampling effort has several unique aspects that make the results especially useful to the emerging field of winter limnology. First, Winter Grab covered a large spatial scale, with 49 sites sampled across all five of the Great Lakes and some of their connecting waters, and most samples collected within 1 week of each other. This broad scale provides an unprecedented snapshot of winter conditions and their variability in a large freshwater ecosystem. Second, our study sites spanned large gradients of trophic status, depth, and ice cover conditions, enabling comparison of winter ecosystem function across these environmental gradients. Third, by collaboratively analyzing samples, we were able to collect data on a broad range of environmental parameters, including physical observations on the properties of ice and the water column, biogeochemical characterization of the water, assessment of bacterioplankton, phytoplankton, and zooplankton communities, and measurements of bacterial and primary production rates. This diversity of location- and time-matched observations provides a comprehensive view of the state of the Great Lakes ecosystem in midwinter, and allows examination of linkages between physical, chemical, and biological processes beyond those that more narrowly focused studies can provide.

In this contribution, we describe the sampling and analytical methods used in the Winter Grab project, provide a detailed overview of the data, identify remaining data gaps, and make recommendations for data use. Our hope is that these data will be useful to a diverse set of researchers trying to integrate winter into understanding of the full year physics, biogeochemistry, and biology of the Laurentian Great Lakes, other large and small lakes, and coastal marine ecosystems.

Data description

The Winter Grab dataset (Pu et al. 2024) is hosted on the Environmental Data Initiative data portal. The dataset is composed of 27 data files in csv format, describing various physical, chemical, and biological parameters for the 49 locations sampled as part of Winter Grab (Table 1). In addition, one metadata file ("WinterGrab_sites") in csv format in Pu et al. (2024) provides site information metadata (Table 2). All Winter Grab dataset files can be joined using the common site name ("station") column.

Sampling sites (Table 2; Fig. 1) spanned a wide range of depths, distances from shore, and trophic status. Because of variations in gear available to different research groups, throughput limitations of effort-intensive measurements such as bacterial and phytoplankton production rates, and lost samples, not all measurements were performed for all sites. For example, chlorophyll *a* (Chl *a*) determinations were made for almost all 49 locations (Table 1; Table 3); conversely, net primary production (NPP) rates were determined only for 11 sites. At sites deeper than ~ 3 m, water chemistry and biological samples were collected just below the ice surface and 1 m above the sediment bottom, allowing for examination of depth variation. The physical observations include multiparameter sonde profiles, ice and snow properties, and observations on light transmission through snow, ice, and the water column. Chemical observations include data on alkalinity, concentrations of total and dissolved forms of phosphorus and nitrogen, chloride concentrations, and dissolved organic matter (DOM) concentrations and forms. Biological observations include Chl *a*, phycocyanin, and phycoerythrin concentrations, concentrations of microcystin (determined by enzyme-linked immunosorbent assay [ELISA]) and cyanotoxin metabolites (determined by LC–MS (Liquid Chromatography Mass Spectrometry)), bacterial abundances determined by flow cytometry and direct counts, phytoplankton abundance and taxonomic composition determined by microscopy, microzooplankton counts and taxonomy determined by microscopy, crustacean zooplankton counts and taxonomy determined by microscopy, and bacterial and phytoplankton production rates, determined by radiolabeled tracer incorporation in lab incubations. Most data files are arranged in a consistent "long" format, with columns corresponding to variables and rows to samples. Summary statistics for selected environmental parameters are shown in Table 4 and Fig. 2, which includes minimum, mean, maximum, and standard deviation.

Methods

Field methods

Sampling locations

Forty-nine locations across all five of the Great Lakes (including some connecting waters, of Lake St. Clair,

Table 1. Summary of all parameters and corresponding categories, filenames, and descriptions.

Category	Parameter name(s)	File name	Description
Physical parameters	CTD	WinterGrab_CTD_profiles.csv	Depth-resolved multiparameter sonde profile data for 16 of our 49 sites.
	Light transmission	WinterGrab_light_transmission.csv	Light (PAR) transmission data through ice and snow, PAR attenuation coefficients through the water column, and descriptions of the ice and snow conditions for 24 of our 49 sites.
	Snow and ice	WinterGrab_snow_ice_properties.csv	Information on ice and snow thickness and properties for 45 of our 49 sampling sites.
Chemical parameters	Alkalinity	WinterGrab_alkalinity.csv	Alkalinity data for 31 of our 49 sites, determined using titration and expressed as micromole per kilogram.
	Chloride	WinterGrab_chloride_concentration.csv	Chloride concentration results for 47 of our 49 sites. Chloride concentrations were determined by potentiometry and are reported as parts per million (ppm).
	DOC and DOM	WinterGrab_DOC_DOM_concentration.csv	DOC concentrations and several parameters characterizing DOM in water and ice samples from 27 (water) and 20 (ice) sites out of our 49 study sites.
	NH_4	WinterGrab_NH4_concentration.csv	Ammonia (NH_4) concentration data from 46 of our 49 sampling sites, determined using the alkaline phenate method and expressed in mg L^{-1}.
	NO_2	WinterGrab_NO2_concentration.csv	Nitrite (NO_2) concentration data for 46 of our 49 sampling sites, determined using cadmium coil reduction followed by sulfanilamide reaction and expressed in mg L^{-1}.
	NO_3	WinterGrab_NO3_concentration.csv	Nitrate (NO_3) concentration data for 46 of our 49 sampling sites, determined using cadmium coil reduction followed by sulfanilamide reaction and expressed in mg L^{-1}.
	Total dissolved phosphorus	WinterGrab_TDP_concentration.csv	TDP concentration data for 46 of our 49 sampling sites, determined by semi-automated colorimetry and expressed in μg L^{-1}.
	Total nitrogen	WinterGrab_TN_concentration.csv	TN concentration data for 46 of our 49 sampling sites, determined using the colorimetric hydrazine method and expressed in mg L^{-1}.
	Total phosphorus	WinterGrab_TP_concentration.csv	TP concentration data for 48 of our 49 sampling sites, determined by semi-automated colorimetry and expressed in μg L^{-1}. Note: Issues with calibration during analysis make these data unsuitable for comparison with TP data from other studies (*see* "Methods" section for additional information).

(Continues)

Table 1. Continued

Category	Parameter name(s)	File name	Description
Biological parameters	Bacterial production rate	WinterGrab_bacterialproduction_rate.csv	BP rate data for water surface samples at 20 of our 49 sites. BP was determined using tritium-labeled methyl-thymidine and leucine incorporation and results are given for both, as either nmol thymidine (or leucine) L^{-1} d^{-1} or in units of ng carbon L^{-1} d^{-1}.
	Chl *a*	WinterGrab_chlA_concentration.csv	Chlorophyll *a* concentration results for 47 of our 49 sites. Chlorophyll *a* concentrations were determined by fluorimetry from acetone-extracted filters and are reported in μg L^{-1}.
	Crustacean zooplankton abundances	WinterGrab_crustacean_zooplankton_abundance.csv	Crustacean zooplankton abundances for 12 of our 49 study sites, in "long" format. Zooplankton abundance was determined by microscopy on zooplankton net tows. Abundances are expressed as individuals per liter.
	Microbial loop components	WinterGrab_microbial_loop_abundance.csv	Abundances of microbial loop components (bacteria, picoplankton, nanoflagellates) determined by microscopy for 11 of our 49 sites, and expressed as cells L^{-1}.
	Microcystin concentration	WinterGrab_microcystin_concentration.csv	Microcystin concentration data for 20 of our 49 sites, as determined by ELISA and expressed in μg L^{-1}.
	Phycocyanin and phycoerythrin concentration	WinterGrab_PCPE_concentration.csv	Phycocyanin (PC) and phycoerythrin (PE) concentration for 21 of our 49 sampling sites. PC and PE concentrations were determined using spectrophotometery and expressed in μg L^{-1}.
	Phytoplankton abundance	WinterGrab_phytoplankton_abundance_McKay.csv	Phytoplankton abundance data for 27 of our 49 sampling sites, determined by the McKay lab (University of Windsor) and expressed in cells mL^{-1}. These data are in "long" format.
	Phytoplankton abundance	WinterGrab_phytoplankton_abundance_Munawar.csv	Phytoplankton abundance data for 13 of our 49 sampling sites, determined by Hedy J. Kling, contracted by the Munawar lab (DFO) and expressed in cells L^{-1}. These data are in "long" format.
	Phytoplankton biomass	WinterGrab_phytoplankton_biomass_Munawar.csv	Phytoplankton biomass data for 13 of our 49 sampling sites, determined by Hedy J. Kling, contracted by the Munawar lab (DFO) and expressed as milligrams wet weight per cubic meter. These data are in "long" format.
	Ciliated protists abundance	WinterGrab_ciliated_protist_abundance.csv	Abundance data on ciliated protists for 24 of our 49 sampling sites, expressed in cells mL^{-1}. These data are in "long" format.

(Continues)

Table 1. Continued

Category	Parameter name(s)	File name	Description
	Microbe abundance	WinterGrab_microbial_flowcytometry_abundance.csv	Microbe abundance data for 44 of our 49 sampling sites, determined using flow cytometry and expressed in cells L^{-1}.
	Cyanotoxin metabolites concentrations	WinterGrab_particulate_cyanotoxins_concentration.csv	Particulate concentrations of 25 cyanotoxin metabolites for 19 of our 49 study sites. Concentrations were determined using liquid chromatography tandem mass spectrometry (LC–MS–MS) for material retained on filters, representing particulate metabolite concentrations, expressed in parts per billion. These data are in "long" format.
Biological parameters	Whole water cyanotoxin metabolites concentrations	WinterGrab_wholewater_cyanotoxins_concentration.csv	Whole water concentrations of 25 cyanotoxin metabolites for 19 of our 49 study sites. Concentrations were determined using liquid chromatography tandem mass spectrometry (LC–MS–MS) for whole water samples, expressed in parts per billion. These data are in "long" format.
	Lab-based phytoplankton primary production rate	WinterGrab_PPR.csv	Phytoplankton primary production rate parameters from measurements performed on samples from 11 of our 49 study sites.
Site metadata	• Sampling site name • PI name • Longitude • Latitude • Sampling dates • Sampling organization • Water depth • Ice thickness • Snow thickness	WinterGrab_sites.csv	Winter grab sampling site metadata, including all 49 site names, locations, and sampling dates. This file can be joined with each data file mentioned above using the "sample site name" column. This file contains all information shown in Table 2.

Table 2. Winter Grab sampling site metadata, water depth, ice thickness, and snow thickness.

Sampling site name	PI	Longitude	Latitude	Sampling dates	Sampling organization	Water depth (m)	Ice thickness (m)	Snow thickness (cm)
Apostles	Ozersky	−90.779	46.837	16 Feb 2022	University of Minnesota Duluth	36.3	0.40	10
BI_Birch_Island	McGregor_Twiss	−81.769	46.066	15 Feb 2022	Algoma University	3	0.46	10
BQ1	Maggie_Xenopoulos_&_Nolan_Pearce	−77.316	44.151	15 Feb 2022	Trent University	10	0.33	0
Bronte_Pier	Warren_Currie	−79.706	43.393	22 Feb 2022	Fisheries and Oceans Canada	4	0	0
CCIW_Hamilton_Harbor	Warren_Currie	−79.802	43.297	16 Feb 2022	Fisheries and Oceans Canada	8	0	0
Eagle_Bay_Saginaw_Bay	Uzarski	−83.877	43.952	22 Feb 2022	Central Michigan University	0.8	0.38	0
EC_1	McKay	−82.392	43.09	28 Feb 2022	University of Windsor	9.5	NA	NA
GR001	McKay	−83.034	41.894	10 Mar 2022	University of Windsor	9.9	0.14	NA
EC_1156	McKay	−83.135	42.054	25 Feb 2022	University of Windsor	11	0	0
EC_12	McKay	−82.054	43.887	10 Mar 2022	University of Windsor	92.8	0	0
EC_1326	McKay	−81.936	41.736	27 Feb 2022	University of Windsor	24.6	0	0
EC_3	McKay	−82.036	43.254	10 Mar 2022	University of Windsor	10.2	0	0
EC_341	McKay	−82.291	41.799	27 Feb 2022	University of Windsor	18.2	0.01	0
EC_84	McKay	−81.637	41.832	27 Feb 2022	University of Windsor	27.7	0.01	0
EC_9	McKay	−82.217	43.633	10 Mar 2022	University of Windsor	63.9	0	0
EC_970	McKay	−82.973	41.826	10 Feb 2022	University of Windsor	11.0	0.14	0
ER_78M	McKay	−81.253	42.106	27 Feb 2022	University of Windsor	24.1	0	0
ER_91M	McKay	−82.905	41.845	10 Feb 2022	University of Windsor	11.1	0.09	0
GB1	Xenopoulos_&_Nolan_Pearce	−79.818	44.773	16 Feb 2022	Trent University	7.9	0.45	1.3
Green_Bay	Ozersky	−87.801	44.64	14 Feb 2022	University of Minnesota Duluth	5.5	0.50	0
Keweenaw_Bay_KB	Vick-Majors	−88.462	46.787	20 Feb 2022	Michigan Technological University	18.6	0.25	2.5
Keweenaw_Waterway_KW	Vick-Majors	−88.546	47.121	17 Feb 2022	Michigan Technological University	5.6	0.33	5
LC_Little_Current	McGregor_Twiss	−81.914	45.981		Algoma University	1.0	0	0
Lorain	Eveleth	−82.175	41.473	15 Feb 2022	Oberlin College	3.0	0.22	6.5
LSC-MB	McKay_Drouillard	−82.421	42.467	15 Feb 2022	University of Windsor	1.4	0.40	1
NB22-002	McKay_Bullerjahn	−82.404	41.515	04 Feb 2022	University of Windsor/ Bowling Green State University	NA	NA	0
NB22-003	McKay_Bullerjahn	−82.963	41.903	04 Feb 2022		NA	NA	NA

(Continues)

Table 2. Continued

Sampling site name	PI	Longitude	Latitude	Sampling dates	Sampling organization	Water depth (m)	Ice thickness (m)	Snow thickness (cm)
					University of Windsor/ Bowling Green State University			
NB22-004	McKay_Bullerjahn	−82.789	41.89	05 Feb 2022	University of Windsor/ Bowling Green State University	NA	NA	NA
NB22-005	McKay	−82.078	41.665	10 Mar 2022	University of Windsor	NA	0	0
NB22-006	McKay	−82.64	41.879	10 Mar 2022	University of Windsor	NA	0	0
NB22-007	McKay	−82.832	41.893	10 Mar 2022	University of Windsor	NA	0	0
NB22-008	McKay	−83.114	41.938	10 Mar 2022	University of Windsor	NA	0	0
Ontario_-_St._Catharines	Bramburger	−79.264	43.21	20 Feb 2022	Environment and Climate Change Canada	2.0	0	0
Parry_Sound_Georgian_Bay	Depew	−80.045	45.342	24 Feb 2022	Environment and Climate Change Canada	24.0	0.32	1
Pinconning_Park_Saginaw_Bay	Uzarski	−83.917	43.85	15 Feb 2022	Central Michigan University	1.6	0.33	0.5
RD_Bay_of_Islands_Whitefish_Falls	McGregor_Twiss	−81.824	46.104	15 Feb 2022	Algoma University	3.0	0.46	10
RW_Ridgeway_Abino_Bay	Zastepa	−79.09	42.848	21 Feb 2022	Environment and Climate Change Canada	1.0	0	0
Saginaw_River*	Karpovich	−83.871	43.614	16 Feb 2022	Saginaw Valley State University	8.5	0.3	0
Saint_Martin_Bay_SM-LH	Doubek	−84.641	46.013	17 Feb 2022	Lake Superior State University	9.7	0.4	1.8
Sandusky_Bay	Bullerjahn_McKay	−82.832	41.497	09 Feb 2022	Bowling Green State University/University of Windsor	1.0	0.15	0
SB1	Godwin	−83.661	43.64	15 Feb 2022	Cooperative Institute for Great Lakes Research	3.2	0.39	1.5
SB14	Godwin	−83.64	43.737	15 Feb 2022	Cooperative Institute for Great Lakes Research	3.7	0.48	0.008
Silver_Harbor _Thunder_Bay	Rennie	−88.973	48.508	19 Feb 2022	Lakehead University	10.5	0.62	9.4
South_Bass_Island	Chaffin	−82.83	41.66	15 Feb 2022	Ohio State University	10.2	0.27	0.01
U17	Twiss	−74.795	45.006	16 Feb 2022	Algoma University	10.0	NA	NA
Vanderbilt_Park_Saginaw_Bay	Uzarski	−83.661	43.61	15 Feb 2022		2.4	0.43	0.4

(Continues)

Table 2. Continued

Sampling site name	PI	Longitude	Latitude	Sampling dates	Sampling organization	Water depth (m)	Ice thickness (m)	Snow thickness (cm)
					Central Michigan University			
WE6	Vanderploeg	−83.386	41.705	14 Feb 2022	NOAA Great Lakes Environmental Research Laboratory	2.8	0.24	0.08
Whitefish_Bay_WB-LS	Doubek	−84.83	46.454	22 Feb 2022	Lake Superior State University	9.9	0.30	9.8
WP_Waverly_Beach_Park	Zastepa	−78.939	42.883	28 Feb 2022	Environment and Climate Change Canada	1.0	0.05	2

NA, no data.
*One site that is in tributaries rather than boundary waters of the Great Lakes system.

Keweenaw Waterway, Saginaw River, and St. Lawrence River) were sampled as part of Winter Grab (Fig. 1; Table 2). Study sites were mostly accessed from shore over ice by foot, ATV, snowmobile, or airboat, but some ice-free locations were sampled from the end of piers and, in the case of the Upper St Lawrence River, within a hydropower dam. A set of 22, mostly pelagic sites were sampled with assistance of US and Canadian Coast Guard (from the USCGC *Neah Bay*, CCGS *Griffon*, and CCGS *Samuel Risley*). Sampling sites ranged in depth from ∼ 1 to 93 m. Of the 49 sites, 32 were ice covered and 17 were ice free. Sampling locations were chosen based on reasonably easy and safe access, and the sites represented gradients of depths, trophic states, and ice cover conditions (Table 2). Absence of stable ice cover and other logistical challenges resulted in only one Lake Michigan site being sampled (in eutrophic Green Bay), representing a gap in the spatial coverage of the dataset. Most sites (83%) were sampled over a 24 d period in February 2022 (04 February 2022 to 28 February 2022); eight mainly pelagic locations were sampled from the US and Canadian Coast Guard icebreakers *Neah Bay* and *Samuel Risley* on 10 March (*see* Table 2 for sampling dates).

Field protocols

At each site, sampling crews recorded coordinates and weather conditions. At sites with ice and snow cover, teams estimated percent snow cover and measured snow depth at five locations in ∼ 10 m radius of the sampling site. If ice was present, sampling crews selected a representative area of snow-covered ice for light attenuation measurements (22 of 49 sites). Using a board to protect snow from slush and water splash, sampling crews augered openings in the ice on the shaded side of the board (facing away from the sun; Fig. 3). Sampling crews then used either a Li-COR Li-192, Li-COR Li-193, or Apogee SQ-500-SS2 photosynthetically active radiation (PAR) sensors to measure light in the air (10 cm above the ice), directly under the ice (pressing the sensor to the underside of the ice on the sun-facing side of the opening in the ice), and then every 50 cm to a depth of 3–5 m. Sampling crews then cleared the snow off the ice (when present) and measured light penetration through the snow-free ice. The hole in the ice was covered by a board or sled during light profiling to minimize light "leakage" through the hole. If no ice was present, light profiles were collected through the water. This approach enabled estimation of light transmission through snow-free ice, snow-covered ice, and the light attenuation coefficients for the water column. Snow and ice thickness and properties are reported in the file WinterGrab_snow_ice_properties.csv. Light transmission through snow and ice, and water attenuation coefficients are reported in the file WinterGrab_light_transmission.csv.

At 17 of the 49 study sites, sampling crews collected water column profiles using CTD sondes. Depending on the sensor suite available to different groups, parameters included water temperature, dissolved oxygen concentration, specific

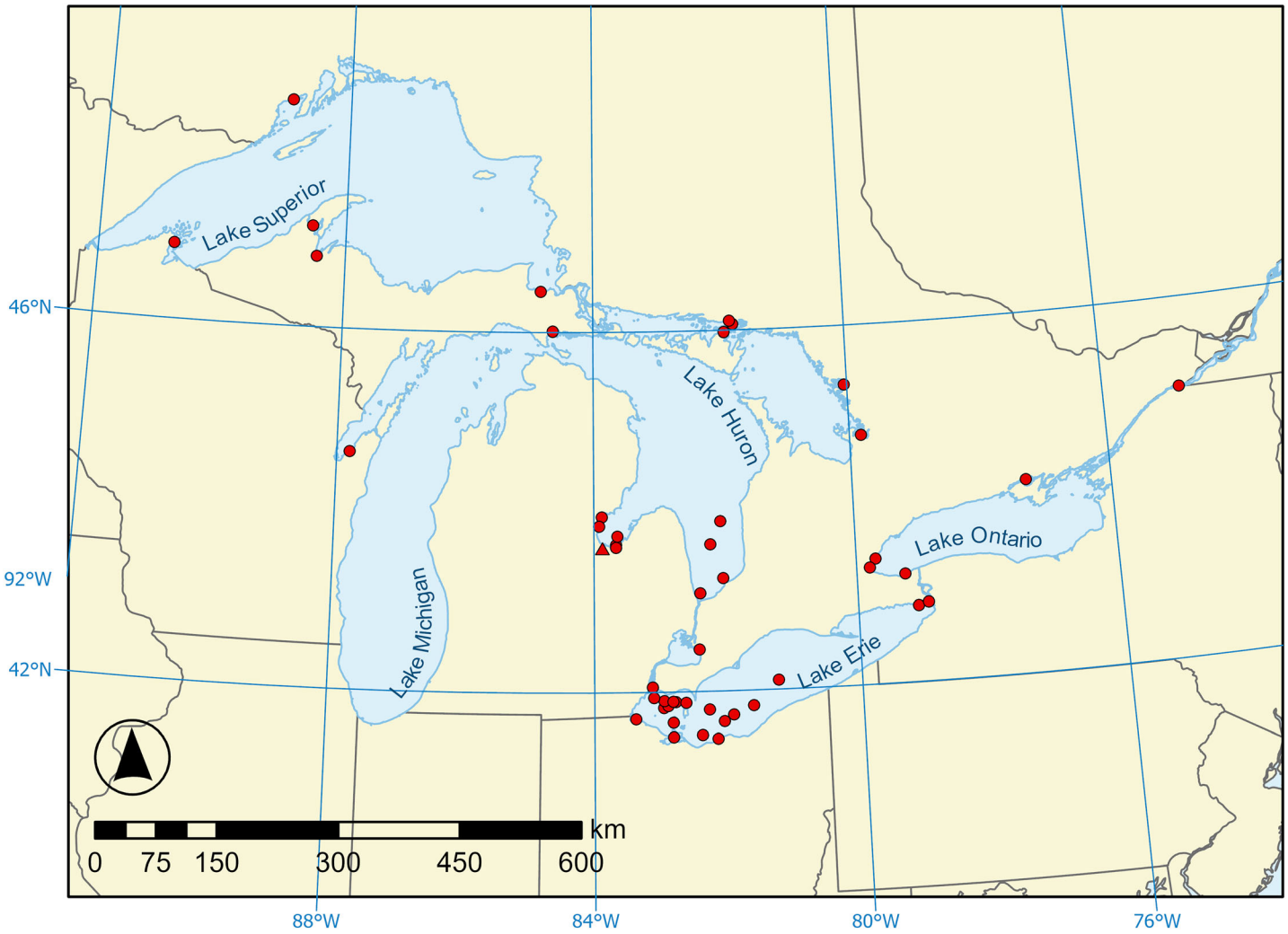


Fig. 1. Map of sampling site locations. Triangle marks one site that is not boundary waters of the Great Lakes but are tributaries.

conductivity, total dissolved solids, and in situ Chl *a* fluorescence. Sondes were lowered at a speed of ~ 0.1 m s^{-1}. If the sonde did not have a continuous recording function, field crews recorded parameters at 0.25 m depth intervals. Sonde profiles are reported in the file WinterGrab_CTD_profiles.csv (Fig. 2).

Where ice was present, field crews augured a separate hole for water and plankton sampling. The hole consisted of three individual round auger holes in a triangle pattern, connected along the sides and with an intact "core" of ice in the middle. The core was removed, the thickness of ice was measured, and any layering recorded. Field crews broke up the ice core, and placed it in clean plastic bags and into a cooler for transport to the lab and later DOM analysis of the ice. Water samples were collected using a Van Dorn or similar sampler. At sites sampled by Coast Guard icebreakers, surface water samples were collected using a stainless steel sampling bottle as described elsewhere (Beall et al. 2016). At sites > 3 m deep, samples were collected from immediately under the ice (or the water surface) and 1 m above the bottom. At shallower sites, only surface water samples were collected. Water samples were placed into acid-cleaned cubitainers or jerricans and kept in the dark and cold until processing within < 8 h after collection.

Crustacean zooplankton samples were collected at 12 sites. Most samples were collected with 64-μm mesh-size zooplankton nets, but some sites were samples with 80- and 153-μm mesh-size zooplankton nets (*see* data file for net parameters at each site). Zooplankton tows were between 1 m above-bottom to the surface. At sites with low zooplankton abundance, several tows were combined into a single sample. Zooplankton samples were preserved in 95% ethanol by volume.

Sample processing

In the lab, water samples were processed for analysis of total phosphorus (TP), total dissolved phosphorus (TDP), total

Table 3. Summary of parameters measured across all Winter Grab sampling sites.

Sampling site name	PI	Phytoplankton biomass	Phytoplankton abundance	Microbial loop abundance	Crustacean zooplankton abundance	Light	Snow ice	NH_4 NO_2 NO_3	Total phosphorus	Total dissolved phosphorus	Chl *a*
Apostles	Ozersky	×	×	×	×	×	×	×	×	×	×
BI_Birch_Island	McGregor_Twiss							×	×	×	×
BQ1	Maggie_×enopoulos_&_Nolan_Pearce	×	×	×	×	×	×	×	×	×	×
Bronte_Pier	Warren_Currie	×	×			×	×	×	×	×	×
CCIW_Hamilton_Harbor	Warren_Currie	×	×	×	×	×	×	×	×	×	×
Eagle_Bay_Saginaw_Bay	Uzarski					×	×		×		
EC_1	McKay	×	×				×	×	×	×	×
GR001	McKay							×	×	×	×
EC_1156	McKay						×		×		×
EC_12	McKay						×	×	×	×	×
EC_1326	McKay						×	×	×	×	×
EC_3	McKay						×	×	×	×	×
EC_341	McKay						×	×	×	×	×
EC_84	McKay	×	×				×	×	×	×	×
EC_9	McKay						×	×	×	×	×
EC_970	McKay						×	×	×	×	×
ER_78M	McKay						×	×	×	×	×
ER_91M	McKay						×	×	×	×	×
GB1	Maggie_×enopoulos_&_Nolan_Pearce	×	×	×	×	×	×	×	×	×	×
Green_Bay	Ozersky	×	×	×	×	×	×	×	×	×	×
Keweenaw_Bay_KB	Vick-Majors				×	×	×	×	×	×	×
Keweenaw_Waterway_KW	Vick-Majors	×	×			×	×	×	×		×
LC_Little_Current	McGregor_Twiss			×				×	×	×	×
Lorain	Eveleth					×	×	×	×	×	×
LSC-MB	McKay_Drouillard	×	×	×		×	×	×	×	×	×
NB22-002	McKay_Bullerjahn						×	×	×	×	×
NB22-003	McKay_Bullerjahn							×	×	×	×
NB22-004	McKay_Bullerjahn							×	×	×	×
NB22-005	McKay						×	×	×	×	
NB22-006	McKay						×	×	×	×	
NB22-007	McKay						×	×	×	×	
NB22-008	McKay						×				
Ontario_-_St._Catharines	Bramburger			×				×	×	×	×
Parry_Sound_Georgian_Bay	Depew						×	×		×	×
Pinconning_Park_Saginaw_Bay	Uzarski					×	×	×	×	×	×
RD_Bay_of_Islands_Whitefish_Falls	McGregor_Twiss							×	×	×	×
RW_Ridgeway_Abino_Bay	Zastepa				×	×	×	×	×	×	×
Saginaw_River*	Karpovich					×	×	×	×	×	×
Saint_Martin_Bay_SM-LH	Doubek				×	×	×	×		×	×
Sandusky_Bay	Bullerjahn_McKay	×	×	×		×	×	×	×	×	×
SB1	Godwin				×	×	×	×	×		×
SB14	Godwin					×	×	×	×	×	×
Silver_Harbor_Thunder_Bay	Rennie					×	×	×	×	×	×
South_Bass_Island	Chaffin	×	×	×	×	×	×	×	×	×	×
U17	Twiss							×	×	×	×

(Continues)

Table 3. Continued

Sampling site name	PI	Phytoplankton biomass	Phytoplankton abundance	Microbial loop abundance	Crustacean zooplankton abundance	Light	Snow ice	NH_4 NO_2 NO_3	Total phosphorus	Total dissolved phosphorus	Chl *a*
Vanderbilt_Park_Saginaw_Bay	Uzarski	×	×	×		×	×	×	×	×	×
WE6	Vanderploeg				×	×	×	×	×	×	×
Whitefish_Bay_WB-LS	Doubek				×	×	×	×	×	×	×
WP_Waverly_Beach_Park	Zastepa					×	×	×	×	×	×

Sampling_Site_Name	PI	DOC and DOM	Alkalinity	Phytoplankton abundance	Phycocyanin and phycoerythrin	Bacterial production	Whole water microcystin	Chloride	CiliatedProtist	Flow cytometry	Net primary	CTD
Apostles	Ozersky	×	×	×	×	×	×	×	×	×	×	
BI_Birch_Island	McGregor_Twiss		×			×		×	×	×		
BQ1	Maggie_×enopoulos_&_Nolan_Pearce	×	×	×	×	×	×	×	×	×		×
Bronte_Pier	Warren_Currie	×	×		×	×	×	×	×	×		×
CCIW_Hamilton_Harbor	Warren_Currie	×	×	×	×	×	×	×	×	×		×
Eagle_Bay_Saginaw_Bay	Uzarski							×			×	×
EC_1	McKay	×	×	×		×		×		×		
GR001	McKay		×	×				×				
EC_1156	McKay	×		×				×				
EC_12	McKay		×	×				×		×		
EC_1326	McKay		×	×				×		×		
EC_3	McKay		×	×				×		×		
EC_341	McKay	×	×	×				×		×		
EC_84	McKay	×	×	×		×		×		×		
EC_9	McKay	×	×	×				×		×		
EC_970	McKay		×	×				×				
ER_78M	McKay		×	×		×		×		×		
ER_91M	McKay		×					×				
GB1	Maggie_×enopoulos_&_Nolan_Pearce	×	×		×	×	×	×	×	×		×
Green_Bay	Ozersky	×	×	×	×	×	×	×	×	×	×	
Keweenaw_Bay_KB	Vick-Majors	×	×	×	×	×	×	×	×	×	×	
Keweenaw_Waterway_KW	Vick-Majors	×	×		×	×	×	×	×	×		×
LC_Little_Current	McGregor_Twiss		×					×	×	×		
Lorain	Eveleth	×	×		×		×	×	×	×		×
LSC-MB	McKay_Drouillard	×		×		×		×		×		
NB22-002	McKay_Bullerjahn		×	×				×		×		
NB22-003	McKay_Bullerjahn		×	×				×		×		
NB22-004	McKay_Bullerjahn		×	×				×		×		
NB22-005	McKay		×	×				×		×		
NB22-006	McKay	×	×	×				×		×		
NB22-007	McKay		×	×				×		×		
NB22-008	McKay			×						×		
Ontario_-_St._Catharines	Bramburger		×					×	×	×		
Parry_Sound_Georgian_Bay	Depew		×					×	×	×		
Pinconning_Park_Saginaw_Bay	Uzarski	×			×		×	×	×	×		×
RD_Bay_of_Islands_Whitefish_Falls	McGregor_Twiss		×					×	×	×		
RW_Ridgeway_Abino_Bay	Zastepa		×		×		×	×	×	×		×
Saginaw_River*	Karpovich		×		×		×	×		×		

(Continues)

Table 3. Continued

Sampling_Site_Name	PI	DOC and DOM	Alkalinity	Phytoplankton abundance	Phycocyanin and phycoerythrin	Bacterial production	Whole water microcystin	Chloride	CiliatedProtist	Flow cytometry	Net primary	CTD
Saint_Martin_Bay_SM-LH	Doubek	×				×	×	×	×	×	×	×
Sandusky_Bay	Bullerjahn_McKay	×	×	×		×		×		×		
SB1	Godwin	×	×		×	×	×	×	×	×	×	×
SB14	Godwin	×	×		×	×	×	×		×	×	×
Silver_Harbor_Thunder_Bay	Rennie	×	×		×		×	×	×	×		
South_Bass_Island	Chaffin	×	×		×			×		×	×	×
U17	Twiss	×	×			×		×	×	×	×	
Vanderbilt_Park_Saginaw_Bay	Uzarski	×	×		×			×	×	×		×
WE6	Vanderploeg	×	×	×	×	×	×	×		×	×	×
Whitefish_Bay_WB-LS	Doubek	×	×	×	×	×	×	×	×	×	×	×
WP_Waverly_Beach_Park	Zastepa		×		×		×	×	×	×		×

*One site that is in tributaries rather than boundary waters of the Great Lakes system.

nitrogen (TN), nitrate/nitrite (NO_3/NO_2), ammonium (NH_4), dissolved organic carbon (DOC), DOM composition, Chl *a*, phycocyanin and phycoerythrin, cyanotoxins, microbial counts by flow cytometry, microbial, phytoplankton, microzooplankton and crustacean zooplankton community composition, as well as bacterial and primary production rate measurements. Ice samples were melted and processed for DOC and DOM as described below.

For TN and TP analysis, whole water samples were placed into acid-washed 60-mL High Density Polyethylene (HDPE) bottles and the samples were frozen until analysis at −20°C. Dissolved nutrient samples (TDP, NH_4, NO_3/NO_2) were frozen following filtration through 0.2-μm pore size nitrocellulose syringe filters. Chl *a* from samples was obtained by filtering 60 mL of whole water through 25-mm diameter 0.2-μm pore size nitrocellulose filters. The filters were frozen until extraction and analysis. Alkalinity samples were filtered through 0.45-μm membrane filters into 50-mL centrifuge tubes with no headspace and stored refrigerated at 4°C. Whole water samples for chloride analysis were also dispensed into 50-mL centrifuge tubes and stored refrigerated until analysis. Water DOC samples were filtered through Whatman 47 mm diameter, 0.2-μm pore-size polycarbonate Polycarbonate Track Etch (PCTE) filters and stored refrigerated at 4°C in pre-combusted amber glass bottles. For ice DOC analysis, samples of lake ice were melted slowly in the refrigerator and processed as above. Samples for total cyanotoxin concentrations were dispensed into 20-mL glass scintillation vials and frozen at −20°C until analysis. Particulate cyanotoxin samples were processed by filtering up to 1000 mL of whole lake water into 47-mm diameter Whatman GF/C filters and freezing the filters at −20°C until analysis. All water samples were processed in duplicate, with the exception of total cyanotoxins, which were processed in triplicate, and data for individual replicates are presented in the dataset that accompanies this paper (Pu et al. 2024).

Samples for microbial (bacteria, archaea, protists) cell counts by flow cytometry were preserved using glutaraldehyde; 1 mL samples of whole water were dispensed into 2 mL cryovials containing 5 μL of 25% glutaraldehyde (Electron Microscopy Sciences 16220) in 100 μL milliQ water. Samples were left for 10 min in the dark and then quickly frozen on dry ice, in liquid N_2, or by being placed into a −80°C freezer. For phytoplankton abundance and community composition determination, whole water samples (45 mL) were fixed with Lugol's iodine and stored at room temperature until processing. For microzooplankton abundance and community composition, whole water samples (45 mL volume) were preserved with 5 mL of 37% formalin and stored refrigerated. Samples for NPP and bacterial production (BP) rate measurements were collected from a subset of sites (Table 3). For NPP measurements, ca. 250 mL of whole water was dispensed into acid-cleaned HDPE bottles, the bottles were wrapped in aluminum foil, and samples

Table 4. Summary statistics for selected environmental parameters. Variables (i.e., CTD, taxonomic information, cyanobacterial metabolites) that could not be easily summarized were excluded due to the number of parameters.

Category	Parameter name	Units	Min	Mean	Max	Standard deviation	*n*
Physical parameters	Light transmission through snow and ice	Percent transmission	0.35	7.27	20.48	6.15	10
	Light transmission through ice	Percent transmission	6.09	23.27	53.93	12.82	21
	Light attenuation coefficient through water	m^{-1}	0.17	0.87	4.16	0.89	23
	Snow thickness	cm	0	0.24	10	1.516	22
	Ice thickness	m	0	0.20	0.62	0.19	22
Chemical parameters	Alkalinity	μmol kg^{-1}	339	1899	3348	793.43	62
	Chloride	ppm	2.46	26.36	161.41	30.48	95
	Dissolved organic carbon in water	mg L^{-1}	1.18	3.41	10.22	2.14	41
	Dissolved organic carbon in ice	mg L^{-1}	0.19	0.92	3.25	0.87	19
	NH_4	mg L^{-1}	0.005	0.0534	0.319	0.06	94
	NO_2	mg L^{-1}	0.0032	0.0096	0.0596	0.0114	64
	NO_3	mg L^{-1}	0.046	0.657	4.074	0.794	123
	Total dissolved phosphorus	μg L^{-1}	0	13.08	63.39	13.08	184
	Total nitrogen	mg L^{-1}	0.296	0.958	5.1	0.947	62
	Total phosphorus	μg L^{-1}	3.21	7.53	28.71	5.1	64
Biological parameters	Bacterial production rate (average of leucine and thymidine based results)	ng C $L^{-1}d^{-1}$	308	4055	11,775	3628	40
	Chl *a*	μg L^{-1}	0.043	3.79	32.7	5.78	100
	Crustacean zooplankton abundances	Ind. L^{-1}	0.062	1.48	9.44	2.92	12
	Microbial loop components	mg m^{-3}	263.2	1360.2	2994.7	832.2	14
	Phycocyanin concentration	μg L^{-1}	0.72	2.41	10.13	2.09	35
	Phycoerythrin concentration	μg L^{-1}	2.15	10.66	31.16	7.89	35
	Phytoplankton abundance	Cell L^{-1}	$4.64 * 10^7$	$9.16 * 10^7$	$3.45 * 10^8$	$8.54 * 10^7$	13
	Phytoplankton biomass	mg m^{-3}	38.8	1752.1	16,761.1	4556.4	13
	Ciliated protists abundance	Cells mL^{-1}	0.01	0.055	0.22	0.052	24
	Microbial flow cytometry abundance	Cells mL^{-1}	$4.42 * 10^5$	$2.09 * 10^6$	$7.90 * 10^6$	$1.29 * 10^6$	167

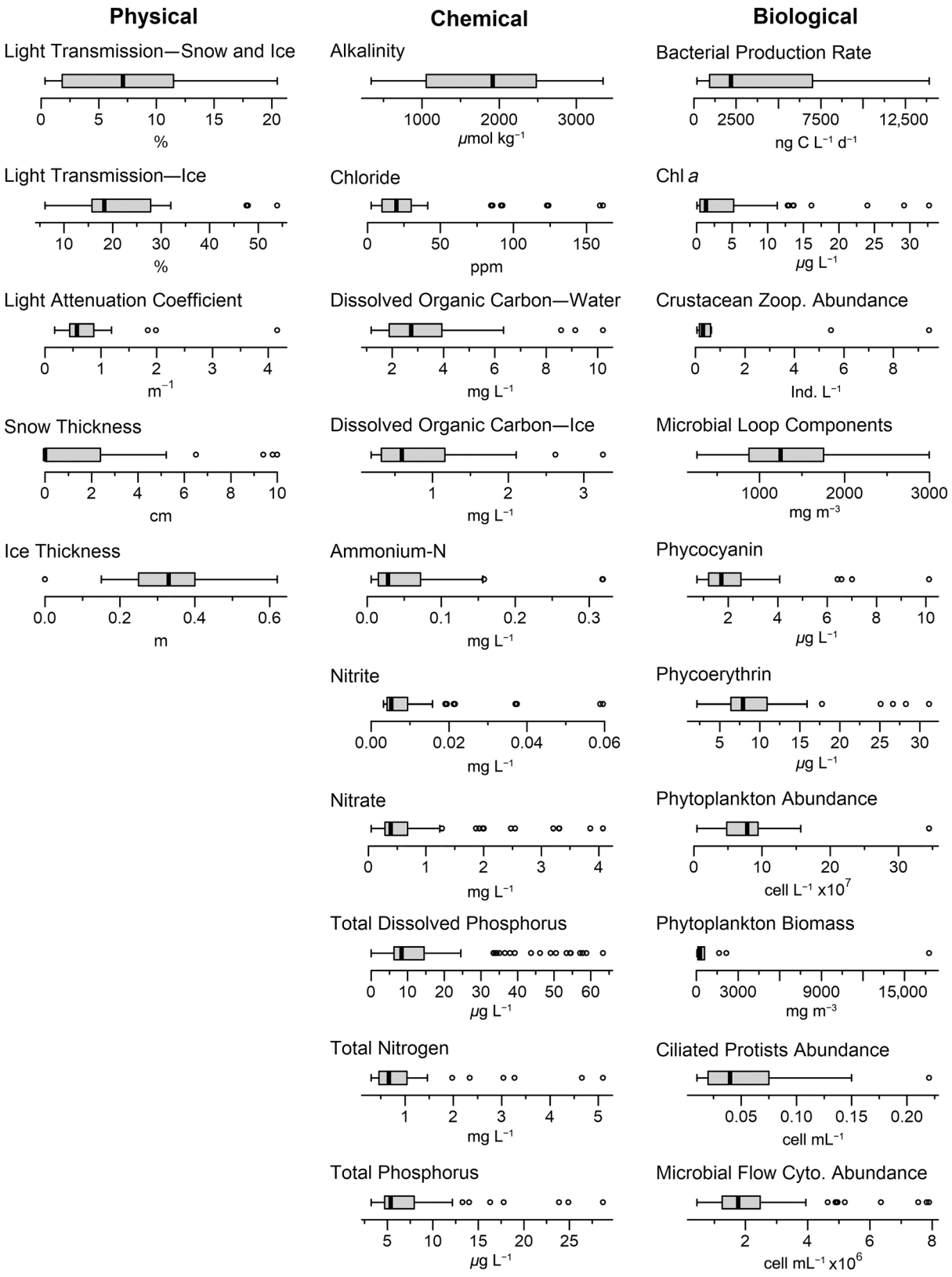


Fig. 2. High Density Polyethylene. Boxplot for selected environmental parameters. Variables (i.e., CTD, taxonomic information, cyanobacterial metabolites) that could not be easily summarized were excluded due to the number of parameters.

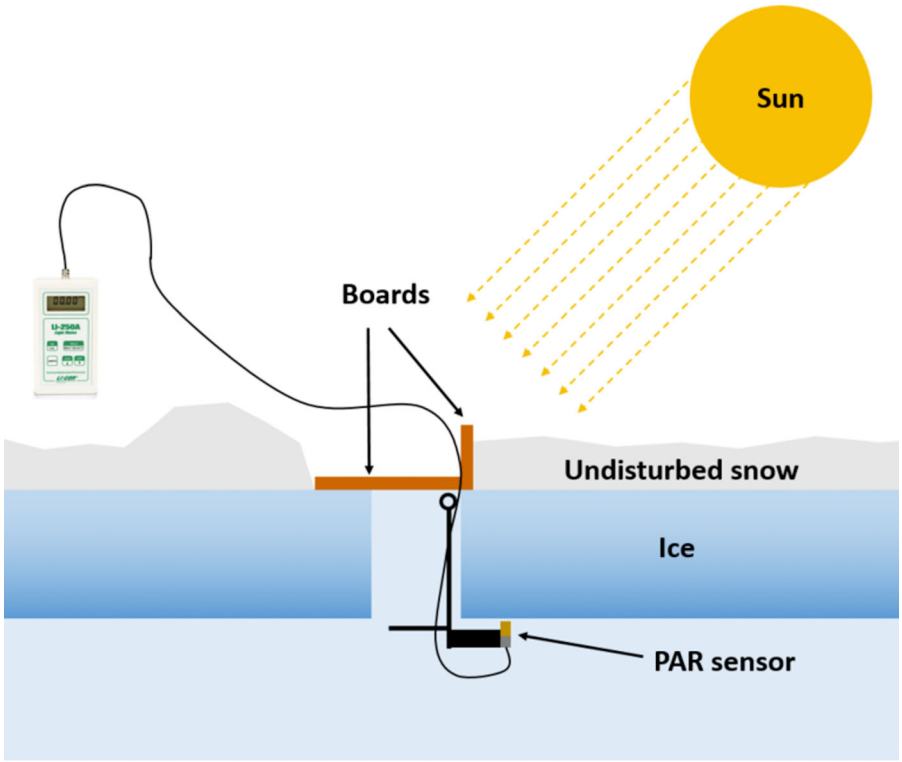


Fig. 3. Diagram showing approach to measuring light penetration through ice and snow cover.

were express-shipped on ice to the Carrick lab at Central Michigan University. For BP measurements, ca. 45 mL of whole water was dispensed into acid-cleaned 50-mL centrifuge tubes, the tubes were wrapped in aluminum foil, and samples were express-shipped on ice to the Vick-Majors lab at Michigan Technological University.

Lab methods

Phosphorus and nitrogen

TP in duplicate whole water samples was determined following persulfate digestion using a modification of EPA method 365.1 (US EPA 1993) on a SEAL AQ-400 discrete analyzer. TDP in duplicate filtered samples was analyzed using the same method as TP. TN in whole (unfiltered), duplicate water samples was analyzed using a flow-injection analyzer (Lachat quickChem 8500 Analyzer), using methods 4500-N and 4500-NO_3-H (APHA 2005). NO_2, NO_3, and NH_4 were also run on the SEAL AQ-400 by using EPA methods 353.2 (US EPA 1993b) and 350.1 (US EPA 1993c), respectively. TP, TDP, NH_4, and NO_3/NO_2 samples were analyzed at the Large Lakes Observatory, University of Minnesota Duluth. Calibration and validation of University of Minnesota Duluth (UMD) analyses were as follows: a 10-point machine calibration, using Hach NIST standards was performed for all analyses. A midrange standard and a milliQ water blank were run at the start of each analytical run and again after every 10–15 samples. In addition to the autoanalyzer-diluted 10-point calibration, a set of 10–15 manual standard dilutions were interspersed throughout the samples and run as "unknown" samples to provide validation. TN samples were analyzed at the National Laboratory for Environmental Testing in Burlington, Ontario. Standards for TN analyses were made using high-purity KNO_3 salt and ultrapure MilliQ water. Seven calibration standards were used to create a calibration curve before every run. High-purity certified nitrate solution (1000 mg L^{-1}—N; from SPEC CertiPrep, Metuchen, NJ 08840) was used as a control solution to verify the stock standard solution. Initial calibration verification was performed using the certified standard every 20 samples. Method blanks consisting of ultrapure MilliQ water were run for each batch. Reference solutions comprised of urea (0.1 mg L^{-1} N), glutamic acid (0.4 mg L^{-1} N), EDTA-di-sodium salt (0.6 mg L^{-1} N), ammonium chloride (0.8 mg L^{-1} N) and water QC standard (0.265 mg L^{-1} N; Lot #8238-10, Phenova) were used to ensure stability of calibrations. TP, TDP, TN, NO_2, NO_3, and NH_4 data are reported in files WinterGrab_TP_concentration.csv, WinterGrab_TDP_concentration.csv, WinterGrab_TN_concentration.csv, WinterGrab_NO2_concentration.csv, WinterGrab_NO3_concentration.csv, WinterGrab_NH4_concentration.csv, respectively.

Alkalinity

Alkalinity was determined on duplicate filtered samples within 3 months of sample collection (Mos et al. 2021). Samples were titrated on a Titrando 888 titrator (Metrohm) using an open-cell two-stage potentiometric titration with 0.1 M HCl following Dickson et al. (2007). Samples were warmed to 25°C prior to analysis and titration was carried out in a water jacketed beaker maintaining that temperature. Alkalinity values were calculated using the Gran approach (Rounds 2012). Alkalinity values of certified reference materials (Batch 200; Dickson 2010) were run at the start of each processing day and were within 5% of expected. Alkalinity was determined at the Eveleth lab at Oberlin College. Alkalinity data are found in the file WinterGrab_alkalinity.csv.

Chloride

Chloride was measured in duplicate unfiltered water samples. Chloride was measured by potentiometry using an ion selective electrode (ISE; Mettler-Toledo chloride combination electrode [perfectION™] connected to a Mettler Toledo Seven Compact voltammeter) on gently stirred samples at room temperature (23°C), with the inclusion of 10 mM M $NaNO_3$ added as an ionic strength adjuster (ISA) for chloride ISE operation in samples and chloride standards of low ionic strength (Mettler-Toledo 2011). A NIST-traceable standard chloride solution (1000 ± 5 ppm Cl^-, as NaCl in water; Thermo Fisher Cat. No. LC-13000-1) was used to establish a standard curve.

Prior to analysis, the chloride ISE was tested for response by determining the slope of the mV detected by 9.7 and 97 ppm Cl^- in deionized water containing 20 mM $NaNO_3$ as ISA. The measured slope was 56.4 mV per 10-fold difference in chloride concentration, which was in the range of 54–60 mV $decade^{-1}$ at 25°C, indicating optimal response by the ISE, as stated by the manufacturer (Mettler-Toledo 2011). Standards of chloride were measured in deionized water containing the same ISA concentrations as samples, and were in the range of 1–101.4 ppm chloride. The mV of the ISE in sample was recorded when the ISE response was stable and the chloride concentration was calculated from the following standard curve established by three repetitions of the standard curve (conducted at the beginning, middle and end of the sample analysis that took place over a 6 h period): $\text{mV sample} = -23.23 \ \ln \ \text{ppm} \ Cl^- + 153.2 \text{ mV}$, $r^2 = 0.995$, $df = 23$. All samples except one (Hamilton Harbor at the CCIW, 6 m depth, 41.2 and 41.4 mV) were within the range of the standards (153.2 [1 ppm Cl^-] to 43.9 mV [101.4 ppm Cl^-]). A comparison of the ISE using the same sonde and methodology described here was made with ion chromatography (IC; EPA Method 300.0) to determine chloride on filtered (< 0.2 μm) water samples from Lake St. Francis (Saint Lawrence River). Chloride analysis by IC was conducted at Paul Smith's College Watershed Institute (certified by the New York State Department of Health's Environmental Laboratory Approval Program, Lab ID no. 12152). The IC analysis was 80.1% ± 2.4% (mean ± SD, $n = 22$) of the value for chloride determined by ISE over a range of chloride (measured by ISE) of 25.3–31.5 ppm chloride. Chloride analysis was performed by MRT at Clarkson University, Potsdam, NY. Chloride data are found in the file WinterGrab_chloride_concentration.csv.

DOC and DOM composition

Filtered (0.2 μm), duplicate water samples, and samples of thawed ice, were analyzed for DOC concentration following persulfate acidification using a Shimadzu Total Organic Carbon Analyzer (TOC-VWP). Spectrofluorometric characteristics of filtered (0.2 μm) samples were further analyzed to characterize DOM composition. DOM absorbance (230–800 nm) was measured with a Varian Cary 50 Bio UV–Visible spectrophotometer and DOM excitation–emission matrices (excitation: 230–500 nm; emission: 270–600 nm) were produced with a Varian Cary Eclipse Fluorometer (Williams et al. 2010). Sample excitation–emission matrices were corrected for instrument bias, inner filter effects, and were blank subtracted then converted to Raman units using a Milli-Q water excitation–emission matrix produced on the day of sample analysis. Five common indices were used to describe DOM composition from absorbance and excitation–emission matrix data: specific ultraviolet light absorbance at 254 nm (SUVA254; Weishaar et al. 2003), spectral slope ratio (Helms et al. 2008), fluorescence index (McKnight et al. 2001), freshness index (β/α; Wilson and Xenopoulos 2009), and humification index (Zsolnay et al. 1999). Furthermore, corrected excitation–emission matrices were fitted to an existing seven-component parallel factor analysis (PARAFAC) model suited to temperate North America using the DOMFluor toolbox (Williams et al. 2016; Williams and Xenopoulos 2023). The proportion and intensity (F_{max}) of PARAFAC components were used to describe DOM composition as ubiquitous humic-like (C1), terrestrial humic-like (C2–C3), soil fulvic-like (C4), microbial humic-like (C5–C6), and/or microbial protein-like (C7). DOM analysis was performed at Xenopoulos Lab at Trent University. DOC/DOM data are in the file WinterGrab_DOC_DOM_concentration.csv.

Pigments: Chl a, phycocyanin, and phycoerythrin

Chl *a* concentrations were determined in duplicate. Chl *a* filters were extracted in 90% acetone solution for 18 h in the dark at 4°C (Welschmeyer 1994). The extracts were run on a Turner Designs 10-AU fluorometer using an excitation wavelength of 436 nm and an emission of 680 nm. The fluorometer is calibrated yearly with manufacturer-supplied liquid calibration standard. In addition, manufacturer-supplied solid low and high standards were used to assess drift and light source stability at the start of each run. Two acetone blanks were analyzed at the start of every run and an additional blank was run every 10 samples. Chl *a* concentration was determined at the Large Lakes Observatory, University of Minnesota Duluth. Chl *a* data are in the file WinterGrab_chlA_concentration.csv.

Phycocyanin and phycoerythrin were extracted and analyzed according to Sarada et al. (1999) and Thoisen et al. (2017), respectively. Cells retained on GF/C filters were ruptured using 3 mL of 50 mM phosphate buffer (pH 6.7, K_2HPO_4) at −4°C for 24 h and then at +4°C for another 24 h to facilitate pigment extraction. The extract was centrifuged (20 min, 5°C, 3210*g* on a Beckman GS-6R centrifuge) to remove the filter and cell debris. Pigments were quantified by measuring the absorbance of the supernatant at 455, 564, 592, and 750 nm on an OceanOptics USB2000 spectrophotometer. Phosphate buffer was used as a blank. The absorbance values were scatter-correct by subtracting the absorbance at 750 nm. To avoid pigment degradation that occurs under exposure to ambient light, red light was used in the laboratory. Phycocyanin and phycoerythrin were measured under the guidance of Arthur Zastepa with McGlynn Laboratories. Phycocyanin and phycoerythrin data are in the file WinterGrab_PCPE_concentration.csv.

Total microcystins extraction and analysis by ELISA

Frozen whole water samples were thawed and a 1 mL aliquot was transferred to a 2-mL microcentrifuge tube, and freeze–thawed for two more times for a total of three freeze–thaw cycles to ensure cell lysis. Samples were centrifuged at 4000 rpm for 3 min and 30 s to remove precipitates, turbidity, and color, and 500 μL of clear supernatant was transferred to a 1.5-mL High Performance Liquid Chromatography (HPLC) amber glass vial and stored in the dark at −80°C until ELISA. Clear samples were not centrifuged after the freeze–thaw steps. Abraxis Microcystins/Nodularins-ADDA ELISA kits (product number 520011) with a detection limit of 0.1 $\mu g\ L^{-1}$ were used following manufacturer's instructions. The kits were stored in the refrigerator at 4°C and allowed to come to room temperature (20–25°C) 30 min before use. The absorbance at 450 nm was read immediately after the last incubation and reagent step using a Biotek microplate spectrophotometer.

The semi-quantitative microcystins concentration of samples were determined by interpolation using a four-parameter logistic standard curve run with each plate. Microsoft Excel was used to calculate mean absorbance values and relative standard deviation of standards, controls, and samples. The % RSD cutoff for confidence in value of standards and controls was < 10%, and the cutoff for samples was < 15%. Samples that had concentrations below the lowest standard (0.15 $\mu g\ L^{-1}$) were reported as below minimum detection limit, and samples with concentrations above the highest standard (5 $\mu g\ L^{-1}$) were diluted and re-run to obtain more accurate results. MilliQ water was used as a diluent for any dilutions required above the upper limit of quantitation (5 $\mu g\ L^{-1}$). Total microcystin analyses were done under the guidance of Arthur Zastepa and the data are in the file WinterGrab_microcystin_concentration.csv.

Total and particulate cyanotoxins and cyanopeptides analyses by mass spectrometry

Particulate cyanotoxins and cyanopeptides were extracted from filters (GF/C, 47 mm, 1.2 μm frozen at −20°C) containing between 250 and 1250 mL of concentrated lake water. Extraction was done using water and methanol (1.6% formic acid). Extraction method details and recovery experiments with fortified samples have been reported in Zastepa et al. (2023). The final 1.5 mL of water-based supernatant was filtered through a 0.45-μm glass fiber filter and transferred to an LC vial for mass spectrometry. Mass spectrometry on whole water (total) cyanotoxins and cyanopeptides was done using the same extract as for ELISA (above), but with a final step of filtering the reconstituted extract through a 0.45-μm glass fiber filter to remove cellular and other debris that could clog the mass spectrometer instrument.

All cyanotoxins and cyanopeptides were analyzed using a Thermo Scientific TSQ Altis™ triple quadrupole mass spectrometer with a TriPlus™ RSH EQuan 850 system; however, different columns were used for subsets of analytes. The loading column, analytical column, chromatographic gradient, mass spectrometer settings, retention times, precursors, and multiple reaction monitoring fragments for each subset have been documented in Zastepa et al. (2023). The method reporting limit for the microcystins and non-microcystin cyanopeptides are less than or equal to 10 $ng\ L^{-1}$ (ppt). More validation information such as standard curve, dynamic range, detection limits, minimum reporting limits, % relative standard deviation, detection limits, and % recovery were also reported in Zastepa et al. (2023). Only whole water samples were tested for saxitoxin and neosaxitoxin because we ran out of standards. Total cyanotoxin analyses were done under the guidance of Arthur Zastepa with Judy A. Westrick and the data are in the file WinterGrab_wholewater_cyanotoxins_concentration.csv. Particulate cyanotoxin data are in the file WinterGrab_particulate_cyanotoxins_concentration.csv.

Bacterial abundance by flow cytometry

Samples for flow cytometry were thawed overnight at 4°C. Samples were diluted 10-fold in 0.2 μm filtered Lake Michigan water and stained with SYBR Green I (Invitrogen) for 30 min at room temperature in the dark (final dye concentration 0.75×). Fluorescent beads (0.5, 1.0, and 2.0 μm yellow–green Fluospheres, Invitrogen) were added to each sample as internal standards. Samples were run on a CytoFLEX S flow cytometer (Beckman Coulter) equipped with violet, blue, and yellow–green lasers. Data acquisition was triggered by side scatter signal and SYBR Green-positive cells were detected by excitation at 488 nm with 525/40 and 585/42 bandpass filters. Samples were run at 10–120 μL per minute depending on concentration. Gating and analysis were performed using CytExpert (Beckman Coulter). Bacterial abundance by flow cytometry data is in the file WinterGrab_microbial_flowcytometry_abundance.csv.

Microbial loop abundance

Microbial loop samples for determination of bacteria, autotrophic picoplankton (APP), and heterotrophic nanoflagellates (HNF) abundances were stored in the refrigerator prior to analysis. Samples were enumerated using 4′,6-diamidino-2-phenylindole (DAPI) staining under epi-fluorescence microscopy (Porter and Feig 1980; Weisse and Munawar 1989). Under reduced lighting (as dark as possible), 5–10 mL of preserved samples was stained with DAPI, filtered through a 0.2-μm nucleopore black filter, and mounted onto a glass slide with a coverslip. Samples not counted immediately were stored in a dark box and kept refrigerated until processing (max. 12 h). After adding immersion oil, samples were counted at 1250× magnification under epifluorescence lighting (excitation wavelength of 365 nm). Following this technique, APP emit red light under green epifluorescence and blue light under UV epifluorescence, whereas bacteria and HNF emit only blue light under UV illumination (Munawar and Munawar 1996). In order to achieve acceptable counting efficiencies, organisms were counted in up to 100 fields of view or until 100 organisms were counted (Lund et al. 1958). Typically, only bacteria reached that threshold and a minimum of 10 fields were always assessed regardless of the cell count. Biomass (wet) was estimated assuming bacteria have a mass of 0.091 pg cell^{-1}, HNF have a mass of 127 pg cell^{-1}, and APP have a mass of 1.82 pg cell^{-1} (Sprules et al. 1999). Microbial loop data are in the file WinterGrab_microbial_loop_abundance.csv.

Phytoplankton abundance and taxonomy

Two groups independently performed phytoplankton counts and taxonomic identification. A set of 27 samples were counted by one group (Mike McKay, University of Windsor) and a set of 13 samples were counted by Hedy J. Kling, contracted by the Mohiuddin Munawar Lab, Fisheries and Oceans Canada. Of these, 9 were counted by both groups, for a total of 32 unique sites. Microscopic identification and enumeration were carried out by the Utermöhl (1958) inverted microscope technique (Munawar and Munawar 1996; Findlay and Kling 1998). A measured aliquot of mixed sample was placed into an inverted microscope counting chamber and allowed to settle a minimum of 4 h per centimeter of overlying water depth. Counting and identification were performed at 125–1000×, depending on the taxon. A minimum of 200 units were counted to achieve an acceptable counting efficiency (Lund et al. 1958). The Windsor group reports results in cells mL^{-1}. The DFO group reported their results as cells L^{-1} and as wet-weight biomass. To determine wet-weight biomass (as mg m^{-3}), cell dimensions were measured directly and the average cell volume for each species was determined by applying the average cell dimensions to a standard geometric shape that most closely resembled the species. In the case of colonial forms, the average number of cells per colony was determined for biomass estimation. Cell volume was converted to wet weight assuming a specific gravity of 1.0 (Strickland 1960). Phytoplankton were identified to the genus level of taxonomic discrimination with some taxa resolved to species level using standard taxonomic sources (*see* Findlay and Kling 1998). The Windsor group generally identified phytoplankton to the genus level, while the DFO group identified phytoplankton to a species level. The difference in taxonomic resolution may have resulted in some of the differences in phytoplankton counts for sites that were counted by the two groups; however, comparing analysis of common samples at genus level and higher showed there to be general alignment with cell abundance within the same order of magnitude. Phytoplankton abundance determined in the McKay lab is in the file WinterGrab_phytoplankton_abundance_McKay.csv. Phytoplankton abundance determined in the Munawar lab is in the file WinterGrab_phytoplankton_abundance_Munawar.csv. Phytoplankton biomass data from the Munawar lab are in the file WinterGrab_phytoplankton_biomass_Munawar.csv.

Ciliated protist abundance and taxonomy

Ciliate abundance and community composition of the microzooplankton assemblage was determined from whole water samples (45 mL volume) that were preserved with 5 mL of 37% formalin and stored refrigerated. Subsequently, these samples were stained with 2% acid Lugol's solution and settled in graduated cylinders for 48 h (1 h per mL sample). After settling, the upper 90 mL was aspirated off, thereby concentrating the sample into a smaller volume (10–12 mL). This material was transferred to vials, and aliquots of the concentrate were placed in counting chambers (3 mL). For each sample, the chamber was initially scanned (20 min) to familiarize the counter with the ciliates present in each sample. Next, the entire contents of the chamber were systematically scanned, so that all ciliated protists present in the sample were identified and their total numbers were enumerated using a research grade, inverted microscope (at 200× magnification Leica 4000). All microzooplankton encountered were identified to the genus level of taxonomic discrimination (*see* Carrick 2005). Ciliated microzooplankton abundance was expressed as individuals per liter (Ind. mL^{-1}). Ciliated microzooplankton abundance was expressed as individuals per liter (Ind. mL^{-1}), and the results are in the file WinterGrab_ciliates_abundance.csv.

Crustacean zooplankton abundance and taxonomy

Subsamples of preserved crustacean zooplankton were transferred into a Bogorov chamber for further counting. Identification and counting were done by using an Olympus SZH10 stereoscopic microscope. Zooplankton identification was based on the key from Balcer et al. (1984) and Haney et al. (2013). Subsamples were counted until at least 200 individuals were identified. Samples with low zooplankton counts (< 200) were concentrated to the lowest possible volume and processed completely. Adult copepods and cladocerans were identified to species level when possible; juvenile copepodites were separated only into cyclopoid and

calanoid groups. We recorded the number of gravid species and counted all nauplii in one group without taxonomic identification. Crustacean zooplankton abundance is expressed as individuals per liter (Ind. L^{-1}), and the results are in the file WinterGrab_crustacean_zooplankton_abundance.csv.

Bacterial and primary production rates

BP rate samples were shipped overnight to Michigan Technological University for measurements and were run as soon as possible after arrival (< 24 h). Heterotrophic BP was measured using [^{3}H]methyl-thymidine incorporation into DNA and [^{3}H]leucine incorporation into protein (Fuhrman and Azam 1982; Kirchman et al. 1985). Samples (1.5 mL; triplicate live and duplicate trichloroacetic acid [TCA] killed controls) amended with a final concentration of 20 nM ^{3}H-thymidine (specific activity 20 Ci $mmol^{-1}$) or ^{3}H-leucine (specific activity 50 Ci $mmol^{-1}$) were incubated in the dark for 4 h at 2°C. Incubations were terminated by the addition of 100% cold TCA (final v/v 5%) and processed by centrifugation and washing with cold 5% TCA (w/v) and 80% ethanol (v/v) to remove cellular debris and unincorporated label. The pellet was dried overnight and amended with 1 mL of Cytoscint ES (MP Biomedicals) and radioactivity determined on a calibrated scintillation counter (Beckman Coulter LS6500). Rates of BP were calculated and converted to units of carbon as described by Vick and Priscu (2012).

Phytoplankton primary production rates were determined at Central Michigan University based on photosynthesis vs. irradiance relationships using a closed incubation system similar to that described by Lewis and Smith (1983). Samples were express-shipped overnight. Upon arrival, water samples were placed in clear, polycarbonate bottles and incubated in a Percival incubator at 4°C and subdued PAR. Experiments were run within 12 h of sample arrival. Collected lake water (70 mL) was dispensed into a 100-mL poly-bottle and inoculated with $NaH^{14}CO3$ (final activity 1 μCi mL^{-1}, Perkin Elmer). Subsamples were dispensed in 19 scintillation vials (20 mL) using a repeat pipettor (3 mL per sample, *see* Fahnenstiel et al. 1989). Eighteen vials were incubated at different levels of PAR in the incubator (incubation time 1 h). One sample was filtered immediately and served as a time zero blank (*see* below). Following incubation, subsamples were concentrated onto membranes (0.7 μm Whatman GF/F) and these were in decontaminated in the vials with 0.5 mL of 0.5 N HCl for 4–6 h in a fume hood (to remove unincorporated $NaH^{14}CO_3$). After decontaminating the samples, counting fluor was added to all scintillation vials (Ecolume, biodegradable). Total activity used in each experiment was determined by taking subsamples from the inoculated water and placing it in vials containing ß-phenylethylamine (Sigma) and counting fluor. All samples were assayed with the Beckman 6500 Scintillation counter using external standards to estimate efficiency and blanks.

Photosynthetic rates were used to construct photosynthesis–irradiance curves using a nonlinear regression curve fitting function (SigmaPlot 12.5, Systat Software) based on the equation of Platt et al. (1980). The model returned three parameters: P_{max}, the maximum photosynthetic rate at light saturation (g C g Chl a^{-1} h^{-1}), α, the slope of the curve at low irradiances (g C g Chl a^{-1} h^{-1} [μmol quanta^{-1} m^{-2}]), and β, the slope of the curve associated with photoinhibition at high irradiance. From these parameters, we could calculate I_k (μmol quanta m^{-2} s^{-1}) to estimate the irradiance at which photosynthesis becomes light-saturated.

Bacterial and primary production rates were determined on samples that were collected at least 24 h before analysis. To reduce bias associated with sample storage and shipping, all samples were shipped in the dark with ice packs and analyzed as soon as possible after arrival. We took additional steps to verify the integrity of samples. For BP rate measurements, we conducted a time-series incubation on freshly collected water from the Keweenaw Waterway (immediately adjacent to the Vick-Majors lab at Michigan Tech) to determine how production rate estimates change during sample storage. Samples were amended with radiolabeled leucine or thymidine as described above and triplicates examined for radioisotope uptake at 2, 4, 6, 12, and 24 h. This experiment demonstrated linearity over the 24 period, indicating that the effect of storage time on these samples should be low (leucine $r^2 = 0.90$, thymidine $r^2 = 0.91$). For primary production rate measurements, each sample was assayed using a Phyto-PAM II fluorometer (Walz) to assess their viability prior to productivity assays. In all cases, samples exhibited photochemical competency with F_m/F_o values greater than 1.0 and yielding significant electron transport response to incremental increase in PAR (all regression slopes > 0). Additionally, tests on the effect of sample storage on Chl *a* concentrations over relevant time scales showed little difference. Given the low in-situ temperatures during sample collection, our careful handling of samples during shipping, and results of the above tests, we believe that bias associated with sample handling and storage was low. Results of BP rate are presented in the file WinterGrab_bacterialproduction_rate.csv. Primary production data are presented in the file WinterGrab_PPR.csv.

Technical validation

Technical validation and quality assurance/control information for individual analyses are included in the lab methods section. Data outliers were identified and when appropriate (e.g., obvious recording error) removed by visually examining data and expert judgment; less than 0.5% of all data were excluded this way. Metadata consistency was checked throughout all data files to maintain the use of the same set of Principal Investigators' names and sampling station names (Table 2). Data column order consistency was also verified following a set of order as close as possible: name of Principal Investigator, name

of sampling station, depth of sample taken, sample names, value of parameter, unit of parameter, and notes.

Data use and recommendations for reuse

Winter limnology is attracting increasing interest from researchers, who are working to address existing data and theory gaps about winter conditions and their role in whole-year ecosystem function. The importance of addressing the winter knowledge gap for the Great Lakes has been recognized by lake management agencies, occasioning the formation of a recent working group on Winter Science by the International Joint Commission (IJC 2024). The data described in this paper represent one of the largest multivariate studies of winter conditions in lakes. These data can be used to explore coupled patterns in biogeochemistry, plankton communities, and productivity rates across large environmental gradients, including trophic status, depth, and ice cover conditions. Beyond advancing understanding of winter limnology in the Laurentian Great Lakes, these data can be incorporated into broader synthesis and meta-analysis efforts by combining them with other winter data from the Laurentian Great Lakes and smaller lakes. In terms of size, physical forcing, and ice regimes, the Laurentian Great Lakes represent an intermediate between lake and marine ecosystems (Sterner et al. 2017), and our winter data may also be of interest to researchers studying winter ecology in coastal marine areas such as the Baltic Sea and ice influenced estuaries. Our data can also be used to calibrate models (e.g., of ice thickness, temperature conditions), as preliminary data for research proposals, and in limnology courses. Finally, these data will be an important baseline for future studies of ecosystem seasonality and long-term change in the Laurentian Great Lakes.

Our dataset has several limitations. Lake Michigan represents an important gap in the spatial coverage of this dataset, with only one site from Lake Michigan's Green Bay sampled during this project. Future efforts should prioritize additional sampling sites in Lake Michigan to provide a more comprehensive understanding of its winter limnology and to ensure this lake is adequately represented in regional and cross-system analyses. Another important limitation of the dataset is the "snapshot" nature of the sampling campaign. Winter conditions are dynamic and change throughout the season. We timed our sampling around the historic period of peak ice cover in the Great Lakes, which we considered "mid-winter." Future work is needed to better understand how the

Table 5. Comparison of our dataset with four other publicly accessible, multivariate datasets on winter limnology of freezing lakes.

Dataset	Year	Lake sampled	# of sites	Description
Pu et al. (2024)	2022	Superior, Michigan, Huron, Erie, Ontario, and connecting waters	49	Physical: water temperature, ice and snow properties, light conditions Chemical: water chemistry, dissolved organic matter characterization Biological: Chl *a* and other pigments, cyanotoxins, plankton abundance and taxonomy, bacterial and primary production
Hampton et al. (2017b)	1982–2008, vary by sites	89 lakes from across North America, Europe, and Antarctica	> 100	Physical: water temperature, ice and snow properties Chemical: water chemistry Biological: Chl *a*, plankton and zoobenthos abundance and taxonomy
Ontario Open Data Team (2020)	1976–2019	Superior, Huron, Erie, and Ontario	18	Chemical: water chemistry Biological: Chl *a*
McKay et al. (2017)	2012, 2013, 2016	Erie	31	Physical: water depth, ice and snow properties, weather, water temperature Chemical: water chemistry Biological: Chl *a*
Bullerjahn et al. (2022)	2018–2020	Erie	30	Physical: water depth, weather, ice and snow properties Chemical: water chemistry Biological: Chl *a*, phytoplankton abundance
Weyhenmeyer et al. (2022)	2021	31 lakes from Europe and North America	31	Physical: snow and ice thickness and characteristics

parameters we examine here change through the winter. Our data are also uneven, with some parameters measured at most sites (e.g., Chl *a* concentrations), and other parameters measured at only a handful of locations (e.g., primary production rates), which limits the ability to assess spatial variation and relationships between parameters. Finally, analyst error during TP analysis resulted in an incorrect calibration curve fitting. As a consequence, the TP data are biased down and represent underestimates of true TP concentrations. While comparisons among sites within the dataset are valid for understanding the relative concentrations of TP across sites, our TP values are not comparable with those of other studies.

Comparison with existing datasets

To our knowledge, this is one of the most extensive (in terms of spatial coverage and number of variables) publicly available datasets of location-matched winter physical, biogeochemical, and biological observations on the Laurentian Great Lakes, or for freshwater ecosystems in general. We are aware of several similar datasets (Table 5). Hampton et al. (2017b), includes diverse winter and summer biogeochemical and plankton biology data for ≤ 122 freshwater lakes (including several Great Lakes locations). The Lake Water Quality at Drinking Water Intakes dataset (Ontario Open Data Team 2020) includes biogeochemical and phytoplankton taxonomic information from 18 drinking water intake plants on the Ontario shores of the Great Lakes. These data have been collected year-round on a ∼biweekly basis since 1976 from some of the plants. McKay et al. (2017) and Bullerjahn et al. (2022) include winter water column physicochemical and phytoplankton abundance data for several dozen sites in Lakes Erie, Huron, and Michigan, including some sites sampled in this work. Using geographical referencing, the above datasets can be combined with our data to provide a broader view of spatial and temporal variation in winter conditions in the Great Lakes and other systems.

References

APHA. 2005. *Standard methods for the examination of water and wastewater*, 21st ed. American Public Health Association/American Water Works Association/Water Environment Federation. doi:10.3390/ijerph2005020017

Balcer, M. D., N. L. Korda, and S. I. Dodson. 1984. *Zooplankton of the Great Lakes: A guide to the identification and ecology of the common crustacean species*. Univ. of Wisconsin Press.

Beall, B. F. N., and others. 2016. Ice cover extent drives phytoplankton and bacterial community structure in a large north-temperate lake: Implications for a warming climate. Environ. Microbiol. **18**: 1704–1719. doi:10.1111/1462-2920.12819

Bullerjahn, G. S., J. T. Anderson, and R. M. McKay. 2022. Winter survey data from Lake Erie from 2018–2020 (Version 4, 25 August 2022). Biological and Chemical Oceanography Data Management Office (BCO-DMO). doi:10.26008/1912/bco-dmo.809945.4

Carrick, H. J. 2005. An under-appreciated component of biodiversity in plankton communities: The role of protozoa in Lake Michigan (a case study). Hydrobiologia **551**: 17–32. doi:10.1007/s10750-005-4447-0

Cavaliere, E., and others. 2021. The lake ice continuum concept: Influence of winter conditions on energy and ecosystem dynamics. J. Geophys. Res. Biogeosci. **126**: e2020JG006165. doi:10.1029/2020JG006165

Chaffin, J. D., and others. 2021. The Lake Erie HABs Grab: A binational collaboration to characterize the western basin cyanobacterial harmful algal blooms at an unprecedented high-resolution spatial scale. Harmful Algae **108**: 80. doi:10.1016/j.hal.2021.102080

Dickson, A. G. 2010. Standards for ocean measurements. Oceanography **23**: 34–47. doi:10.5670/oceanog.2010.22

Dickson, A. G., and others. 2007. *Guide to best practices for ocean CO_2 measurement*. North Pacific Marine Science Organization. doi:10.25607/OBP-1342

Doan, P. T. K., and others. 2018. Phosphorus retention and internal loading in the Bay of Quinte, Lake Ontario, using diagenetic modelling. Sci. Total Environ. **636**: 39–51. doi:10.1016/j.scitotenv.2018.04.252

Dugan, H. A. 2021. A comparison of ecological memory of lake ice-off in eight north-temperate lakes. J. Geophys. Res. Biogeosci. **126**: e2020JG006232. doi:10.1029/2020JG006232

Eadie, B. J., and others. 2002. Particle transport, nutrient cycling, and algal community structure associated with a major winter–spring sediment resuspension event in southern Lake Michigan. J. Great Lakes Res. **28**: 324–337. doi:10.1016/S0380-1330(02)70588-1

Fahnenstiel, G. L., J. F. Chandler, H. J. Carrick, and D. Scavia. 1989. Photosynthetic characteristics of lakes Huron and Michigan phytoplankton communities: P-I parameters and end-products. J. Great Lakes Res. **15**: 394–407. doi:10.1016/S0380-1330(89)71495-7

Farmer, T. M., E. A. Marschall, K. Dabrowski, and S. A. Ludsin. 2015. Short winters threaten temperate fish populations. Nat. Commun. **6**: 7724. doi:10.1038/ncomms8724

Findlay, D. L., and H. J. Kling. 1998. *Protocols for measuring biodiversity: Phytoplankton in freshwater*. Fisheries and Oceans Canada, p. 20.

Fuhrman, J., and F. Azam. 1982. Thymidine incorporation as a measure of heterotrophic bacterioplankton production in marine surface waters: Evaluation and field results. Mar. Biol. **66**: 109–120. doi:10.1007/BF00397184

Hampton, S. E., A. W. Galloway, S. M. Powers, T. Ozersky, K. H. Woo, R. D. Batt, and M. A. Xenopoulos. 2017*a*. Ecology under lake ice. Ecol. Lett. **20**: 98–111. doi:10.1111/ele.12699

Hampton, S., and others. 2017*b*. Winter and summer comparison of biological, chemical, and physical conditions in

seasonally ice-covered lakes. Knowledge Network for Biocomplexity **136**: 1–19. doi:10.5063/F12V2D1V

Haney, J. F., and others. 2013. *An-image-based key to the zooplankton of North America. Version 5.0*. University of New Hampshire Center for Freshwater Biology, Available from http://cfb.unh.edu/cfbkey/html/references.htm

Helms, J. R., A. Stubbins, J. D. Ritchie, E. C. Minor, D. J. Kieber, and K. Mopper. 2008. Absorption spectral slopes and slope ratios as indicators of molecular weight, source, and photobleaching of chromophoric dissolved organic matter. Limnol. Oceanogr. **53**: 955–969. doi:10.4319/lo.2008.53.3.0955

International Joint Commission. 2024. Frigid fieldwork: Great lakes winter science. Available from https://www.ijc.org/sites/default/files/SAB%20Winter%20Science%20One%20pager%20-%20final%20digital.pdf

Jansen, J., and others. 2021. Winter limnology: How do hydrodynamics and biogeochemistry shape ecosystems under ice? J. Geophys. Res. Biogeosci. **126**: e2020JG006237. doi:10.1029/2020JG006237

Kirchman, D., E. K'nees, and R. Hodson. 1985. Leucine incorporation and its potential as a measure of protein synthesis by bacteria in natural aquatic systems. Appl. Environ. Microbiol. **49**: 599–607. doi:10.1128/aem.49.3.599-607.1985

Kirillin, G., and others. 2012. Physics of seasonally ice-covered lakes: A review. Aquat. Sci. **74**: 659–682. doi:10.1007/s00027-012-0279-y

Knoll, L. B., and others. 2019. Consequences of lake and river ice loss on cultural ecosystem services. Limnol. Oceanogr. Lett. **4**: 119–131. doi:10.1002/lol2.10116

Lewis, M. R., and J. C. Smith. 1983. A small volume, short-incubation-time method for measurement of photosynthesis as a function of incident irradiance. Mar. Ecol. Prog. Ser. **13**: 99–102. doi:10.3354/meps013099

Lund, J. W. G., C. Kipling, and E. D. LeCren. 1958. The inverted microscope method of estimating algal numbers and the statistical basis of estimation by counting. Hydrobiologia **9**: 143–170. doi:10.1007/BF00007865:

McKay, R. M., P. F. Morris, and G. S. Bullerjahn. 2017. Physico-chemical data from winter 2012, 2013, and 2016 from USCGC and CCGS vessels from the Laurentian Great Lakes (mainly lakes Huron, Michigan, Erie and connecting waterways) (Lake Erie Ice project) (Version 2, 18 July 2017). Biological and Chemical Oceanography Data Management Office (BCO-DMO). Available from http://lod.bco-dmo.org/id/dataset/4045

McKnight, D. M., and others. 2001. Spectrofluorometric characterization of dissolved organic matter for indication of precursor organic material and aromaticity. Limnol. Oceanogr. **46**: 38–48. doi:10.4319/lo.2001.46.1.0038

Mettler-Toledo. 2011. *PerfectION™ guidebook - combination chloride electrode successful ion measurement*. Mettler-Toledo AG, Available from www.mt.com

Mos, B., C. Holloway, B. P. Kelaher, I. R. Santos, and S. A. Dworjanyn. 2021. Alkalinity of diverse water samples can be altered by mercury preservation and borosilicate vial storage. Sci. Rep. **11**: 9961. doi:10.1038/s41598-021-89110-w:

Munawar, M., and I. F. Munawar. 1996. *Phytoplankton dynamics in the North American Great Lakes*, v. **1**. Ontario, Erie and St. Clair. Ecovision World Monograph Series. SPB Academic Publishing. doi:10.14321/j.ctt13x0pk1:

Ontario Open Data Team. 2020. Lake water quality at drinking water intakes [Dataset]. Ontario data catalog. Available from: https://data.ontario.ca/dataset/lake-water-quality-at-drinking-water-intakes. doi:10.2500/jfa.2020.2.200015

Ozersky, T., and others. 2021. The changing face of winter: Lessons and questions from the Laurentian Great Lakes. J. Geophys. Res. Biogeosci. **126**: e2021JG006247. doi:10.1029/2021JG006247

Platt, T., C. L. Gallegos, and W. G. Harrison. 1980. Photoinhibition of photosynthesis in natural assemblages of marine phytoplankton. J. Mar. Res. **38**: 687–701. https://elischolar.library.yale.edu/journal_of_marine_research/1525

Porter, K. G., and Y. S. Feig. 1980. The use of DAPI for identifying and counting aquatic microflora 1. Limnol. Oceanogr. **25**: 943–948. doi:10.4319/lo.1980.25.5.0943

Pu, G., and others. 2024. Data package for the 2022 Great Lakes Winter Grab ver 1. Environmental Data Initiative. doi:10.6073/pasta/25b45064d0e2fd8578aad055609c0ca3

Reavie, E. D., and others. 2016. Winter–spring diatom production in Lake Erie is an important driver of summer hypoxia. J. Great Lakes Res. **42**: 608–618. doi:10.1016/j.jglr.2016.02.013

Rounds, S. A. 2012. Chapter A6: Alkalinity and acid neutralizing capacity (Version 4.0). *In* F. D. Wilde and D. B. Radtke [eds.], *National field manual for the collection of water-quality data*, Section 6.6, 45 p. U.S. Geological Survey Techniques of Water-Resources Investigations, Available from http://water.usgs.gov/owq/FieldManual/Chapter6/section6.6/

Salonen, K., M. Leppäranta, M. Viljanen, and R. D. Gulati. 2009. Perspectives in winter limnology: Closing the annual cycle of freezing lakes. Aquat. Ecol. **43**: 609–616. doi:10.1007/s10452-009-9278-z

Sarada, R. M. G. P., M. G. Pillai, and G. A. Ravishankar. 1999. Phycocyanin from spirulina sp: Influence of processing of biomass on phycocyanin yield, analysis of efficacy of extraction methods and stability studies on phycocyanin. Process Biochem. **34**: 795–801. doi:10.1016/S0032-9592(98)00153-8

Serville-Tertullien, M., E. Pirie, M. C. Buell, B. M. Wall, and C. Furgal. 2023. Indigenous peoples-related environmental research within the basin of the Laurentian Great Lakes: A systematic map protocol. Ecol. Solut. Evid. **4**: e12199. doi:10.1002/2688-8319.12199

Sharma, S., and others. 2019. Widespread loss of lake ice around the Northern Hemisphere in a warming world. Nat. Clim. Change **9**: 227–231. doi:10.1038/s41558-018-0393-5

Shchapov, K., and T. Ozersky. 2023. Opening the black box of winter: Full-year dynamics of crustacean zooplankton along a nearshore depth gradient in a large lake. Limnol. Oceanogr. **68**: 1438–1451. doi:10.1002/lno.12355

Sprules, W.G., and others. 2000. Trophie transfer in Lake Erie: a whole food web modeling perspective. In *Great Lakes Modeling Summit: Focus on Lake Erie*. L.A. Tulen and J.V. DePinto, eds., pp. 31-36. Council of Great Lakes Research Managers, International Joint Com- mission, Windsor, ON.

Sterner, R. W., and others. 2017. Grand challenges for research in the Laurentian Great Lakes. Limnol. Oceanogr. **62**: 2510–2523. doi:10.1002/lno.10585

Strickland, J. D. H. 1960. *Measuring the primary production of marine phytoplankton*. Bulletin of Fisheries Research Board of Canada, p. 122.

Thoisen, C., B. W. Hansen, and S. L. Nielsen. 2017. A simple and fast method for extraction and quantification of cryptophyte phycoerythrin. MethodsX **4**: 209–213. doi:10.1016/j.mex.2017.06.002

Twiss, M. R., and others. 2012. Diatoms abound in ice-covered Lake Erie: An investigation of offshore winter limnology in Lake Erie over the period 2007 to 2010. J. Great Lakes Res. **38**: 18–30. doi:10.1016/j.jglr.2011.12.008

U.S. Environmental Protection Agency. 1993*a*. *Method 365.1: Determination of phosphorus by semi-automated colorimetry*. Environmental Monitoring Systems Laboratory.

U.S. Environmental Protection Agency. 1993*b*. *Method 353.2: Determination of nitrate-nitrite nitrogen by automated colorimetry*. Environmental Monitoring Systems Laboratory.

U.S. Environmental Protection Agency. 1993*c*. *Method 350.1: Determination of ammonia nitrogen by semi-automated colorimetry*. Environmental Monitoring Systems Laboratory.

Utermöhl, H. 1958. Zur vervolkommnung der quantitativen phytoplankton-methodik [The improvement of quantitative phytoplankton methodology] (in German). Mitt. Internat. Verein. Limnol. **9**: 1–38. doi:10.1080/05384680.1958.11904091:

Vick, T., and J. Priscu. 2012. Bacterioplankton productivity in lakes of the Taylor Valley, Antarctica, during the polar night transition. Aquat. Microb. Ecol. **68**: 77–90. doi:10.3354/ame01604

Wang, X., and others. 2022. Continuous loss of global lake ice across two centuries revealed by satellite observations and numerical modeling. Geophys. Res. Lett. **49**: e2022GL099022. doi:10.1029/2022GL099022

Weishaar, J. L., G. R. Aiken, B. A. Bergamaschi, M. S. Fram, R. Fujii, and K. Mopper. 2003. Evaluation of specific ultraviolet absorbance as an indicator of the chemical composition and reactivity of dissolved organic carbon. Environ. Sci. Technol. **37**: 4702–4708. doi:10.1021/es030360x

Weisse, T., and M. Munawar. 1989. *Evaluation of the microbial loop in the North American Great Lakes*. *Canadian Technical Report of Fisheries And Aquatic Sciences No. 1709*. Fisheries and Oceans Canada, p. 1–30. https://publications.gc.ca/collections/collection_2014/mpo-dfo/Fs97-6-1709-eng.pdf

Welschmeyer, N. A. 1994. Fluorometric analysis of chlorophyll *a* in the presence of chlorophyll *b* and pheopigments. Limnol. Oceanogr. **39**: 1985–1992. doi:10.4319/lo.1994.39.8.1985

Weyhenmeyer, G. A., and others. 2022. Towards critical white ice conditions in lakes under global warming. Nat. Commun. **13**: 4974. doi:10.1038/s41467-022-32633-1:

Williams, C. J., Y. Yamashita, H. F. Wilson, R. Jaffé, and M. A. Xenopoulos. 2010. Unraveling the role of land use and microbial activity in shaping dissolved organic matter characteristics in stream ecosystems. Limnol. Oceanogr. **55**: 1159–1171. doi:10.4319/lo.2010.55.3.1159

Williams, C. J., P. C. Frost, A. M. Morales-Williams, J. H. Larson, W. B. Richardson, A. S. Chiandet, and M. A. Xenopoulos. 2016. Human activities cause distinct dissolved organic matter composition across freshwater ecosystems. Glob. Change Biol. **22**: 613–626. doi:10.1111/gcb.13094

Williams, C. J., and M. A. Xenopoulos. 2023. 7-Component PARAFAC model, dataset, and matlab code of aquatic dissolved organic matter composition in North American Great Lakes region. figshare. doi:10.6084/m9.figshare.24018450.v2

Wilson, H. F., and M. A. Xenopoulos. 2009. Effects of agricultural land use on the composition of fluvial dissolved organic matter. Nat. Geosci. **2**: 37–41. doi:10.1038/ngeo391

Yang, B., M. G. Wells, J. Li, and J. Young. 2020. Mixing, stratification, and plankton under lake-ice during winter in a large lake: Implications for spring dissolved oxygen levels. Limnol. Oceanogr. **65**: 2713–2729. doi:10.1002/lno.11543

Zastepa, A., J. A. Westrick, A. Liang, J. A. Birbeck, E. Furr, L. C. Watson, J. L. Stockdill, B. S. Ramakrishna, and S. Crevecoeur. 2023. Broad screening of toxic and bioactive metabolites in cyanobacterial and harmful algal blooms in Lake of the Woods (Canada and USA), 2016–2019. J. Great Lakes Res. **49**: 134–146. doi:10.1016/j.jglr.2022.12.006

Zsolnay, A., E. Baigar, M. Jimenez, B. Steinweg, and F. Saccomandi. 1999. Differentiating with fluorescence spectroscopy the sources of dissolved organic matter in soils subjected to drying. Chemosphere **38**: 45–50. doi:10.1016/S0045-6535(98)00166-0

Acknowledgments

We thank the following people for assistance in the field and in the lab: Audrey Huff, Natasha Shchapova (University of Minnesota Duluth), Kevin Kapuscinski (Lake Superior State University), Claire Stevens, Anthony Arsenault, Oghenemise Abirhire (Trent University), George Bullerjahn, Ryan Wagner (Bowling Green State University), Ken Drouillard, Aaron Newhook (University of Windsor), Vanessa Cubillos Tellez, Ethan Miller, Melia Austin, Alayna Merten (Michigan Technological University), Jeff

Elliott (NOAA GLERL), Jason Smith (Bay Mills Indian Community), Keara Stanislawczyk, Autumn Taylor, Art Wolf, Craig Genheimer, Jon Linhart (Ohio State University), Lauren Hayhurst (IISD Experimental Lakes Area), Brenden Slongo (Lakehead University) for assistance with field sampling and laboratory processing, and the School of Natural Resources and the Center for Freshwater Research and Education at LSSU for support for travel and equipment use. Raymond Shane McGregor (deceased) and Clayton Courtney Jr and Sr assisted MRT with sample collection and processing along the North Channel of Lake Huron. We thank members of USCG *Neah Bay*, CCGS *Samuel Risley* and CCGS *Griffon* for the collection of samples from pelagic locations during Winter Grab. The dissolved organic carbon quantity and composition samples were analyzed and processed with funding from Canada's Natural Sciences and Engineering Research Council and Canada Research Chair to MAX. This is contribution 206 of the Central Michigan University Institute for Great Lakes Research, GLERL Contribution No. 2057, and CIGLR contribution number 1226. Additional in-kind funding was provided by all of the participating institutions.

Submitted 29 March 2024
Revised 17 September 2024
Accepted 08 October 2024